ACTIVE AND REACTIVE POWER CONTROL IN AN ISLANDED SOLAR MICROGRID USING DROOP CONTROLLER

A Dissertation submitted in fulfillment of the requirements for the Degree

Of

MASTER OF ENGINEERING

In

Power Systems

Submitted by

Pankaj Verma
801441019

Under the Guidance of
Dr. Prasenjit Basak
Assistant professor, EIED

2016

Electrical and Instrumentation Engineering Department

Thapar University, Patiala

(Declared as Deemed-to-be-University u/s 3 of the UGC Act., 1956)

Post Bag No. 32, Patiala – 147004

Punjab (India)

DECLARATION

I hereby certify that the work which is presented in dissertation entitled, **"Active and Reactive Power Control in an Islanded Solar Microgrid using Droop Controller"**, in fulfillment of the requirements for the award of the degree of Master of Engineering in Power Systems, submitted to Electrical & Instrumentation Engineering Department of Thapar University, Patiala is as authentic record of my own work carried under the supervision of **Dr. Prasenjit Basak.** It refers others researcher's work which are duly listed in the reference section. The matter contained in this dissertation has not been submitted, neither in part or in full to any other degree to any other university or institute except as reported in text and references.

Place: Patiala
Date: 14/07/2016

Pankaj Verma
Roll No: 801441019

It is certified that the above statement made by the student is correct to the best of my knowledge and belief.

Date: 14/7/16

Dr. Prasenjit Basak
Assistant professor
Electrical and Instrumentation Engineering Department
Thapar University, Patiala

Countersigned by:

Dr. Ravinder Agarwal
Professor & Head
Electrical and Instrumentation Engineering Department
Thapar University
Patiala

Dr. S.S.Bhatia
Dean (Academic Affairs)
Thapar University
Patiala

CERTIFICATE

Certified that the dissertation entitled, "**Active and Reactive Power Control in an Islanded Solar Microgrid using Droop Controller**", which is being submitted by **Pankaj Verma** in fulfillment of the requirements for the award of the **Master of Engineering in Power Systems**, to Thapar Institute of Engineering & Technology University, Patiala, is a bonafide record of the candidate's own work carried out by him under my supervision and guidance. The matter contained in this dissertation has not been submitted, neither in part nor in full to any other university or institute for award of any degree.

Place: Patiala

Date: 14/7/16.

(Dr. Prasenjit Basak)

Supervisor

ACKNOWLEDGEMENT

First and foremost I would like to thank Thapar University, Patiala for providing me the scope and resources to successfully submit my dissertation entitled “Active and Reactive Power Control in an Islanded Solar Microgrid using Droop Controller”.

I express my deep gratitude to my supervisor, Dr. Prasenjit Basak who despite his busy schedules was always a source of constant motivation and provided sincere guidance.

I would also like to extend my gratitude to Dr. Ravinder Agarwal (Professor and Head) along with other faculty members and staffs of the department, who have provided valuable support to me during various phases of my dissertation work.

Last but not the least; I would like to thank my parents and friends who have always stood by me irrespective of situations.

Pankaj Verma

Regd. No. 801441019

TABLE OF CONTENTS

LIST OF TABLES

LIST OF FIGURES

NOMENCLATURE

V_{dc} = Dc source voltage.

V_C = Capacitor voltage.

I_C = Capacitor current.

L_f = Filter inductance.

C_f = Filter capacitance.

R_f = Filter resistance.

X_{lfm} = Filter inductive reactance in an equivalent circuit of averaged inverter system.

X_{cfm} = Filter capacitive reactance in an equivalent circuit of averaged inverter system.

R_l = Load resistance in an equivalent circuit of averaged inverter system.

X_{lm} = Load inductive reactance in an equivalent circuit of averaged inverter system.

$e_c(t)$ = Error signal.

I_{SC} = Short circuit current of the PV cell.

I_d = Diode current in the PV cell.

V_{OC} = Open circuit voltage of the PV cell.

R_P = Parallel leakage resistance of the PV cell.

R_S = Series resistance of the PV cell.

V_{SH} = Output voltage of entire module of PV system.

T_{ST} = Standard temperature (25^OC).

T_{AM} = Ambient temperature.

STC = Standard test conditions i.e. 25^OC temperature and 1000 W/m^2 Irradiance.

DG = Distributed generation

V2G = Vehicle to grid system.

PV = Photovoltaic

DER = Distributed energy resources.

THD = Total harmonic distortion.

ABSTRACT

In the study of control configuration of solar microgrid, in most of the cases, operation of the photovoltaic generator is represented considering a dc voltage source equivalent to the output of the photovoltaic generator. In this dissertation, implementation of the mathematical model of a photovoltaic generator is considered in the microgrid configuration which increases the analysis of the same in more practical aspect. Further, a power controller which works based on droop-characteristics is proposed to control the real and reactive power in the islanded mode of microgrid operation. Improved results are observed for control of active and reactive power while the microgrid system is simulated with the proposed controller compared to the performance of the same working without controller. The entire analysis of the proposed solar microgrid model has been performed considering solar insolation, ambient temperature and shading effects of the photovoltaic generator. The model is simulated using Simulink-MATLAB software and found satisfactory results.

CHAPTER 1

INTRODUCTION

1.1 OVERVIEW

The increase in the demand of power is in the direct proportion to the increase in population, as we are at the verge of exhausting most of our non-renewable resources (a typical curve of oil production is shown in Fig. 1) hence the interest in the renewable sources of energy is at its peak. The renewable sources of energy have proved to be useful for fulfilling the power demands. These sources have many forms like wind energy, solar energy, biomass energy etc, but the wind and solar energy have proved to be the most successful way of harnessing power from the renewable energy sources. These sources are also called as microsources.

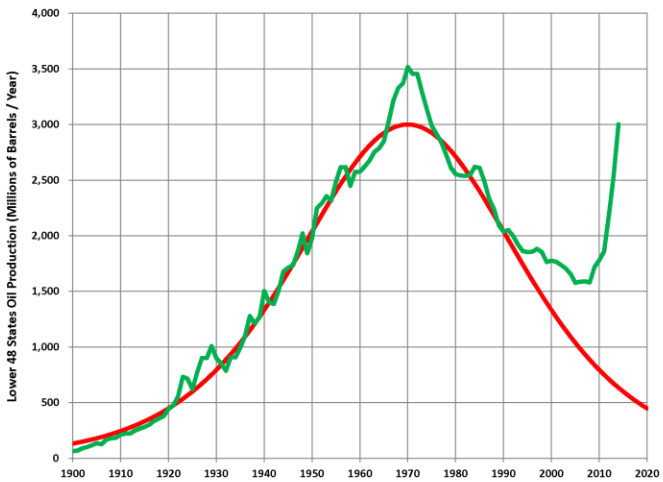

Fig. 1. Yearly oil production curve [1]

The power developed from these microsources is small or in a way the power is distributed. The configuration in which these microsources are combined together to act as a single cell so as to provide the higher power demands is known as the microgrid. Microsources present in the microgrid could be a wind turbine, fuel cell, micro turbine (or small hydel plant), photovoltaic cell or a most advanced concept include the vehicle to grid (V2G) system in which plug in electric vehicles communicate with the power grids [2]. The microsources can be ac microsources or dc microsource e.g. a wind generator can be an ac microsource while photovoltaic generator is a dc microsource. Regardless of the nature of the microsource the

supply from these sources cannot be fed directly to the loads or to the central grid. In case of the dc microsources the dc is first converted to ac using various control configurations [3-8]. In most of these control configurations the dc microsource is considered as the ideal fixed dc source, which is not the same for many microsources.

1.2 MICROGRID

1.2.1 BASIC CONCEPT OF MICROGRID

The configuration in which various distributed sources are combined to serve together is simply a microgrid. Technically, a microgrid is a localized grouping of electricity sources and loads that normally operate connected to the centralized grid, but can disconnect and function autonomously as physical and/or economic conditions dictate. The microgrid is a logical evolution of simple distribution networks and can accommodate a high density of various distributed generation sources. A typical microgrid power system consists of generators, wind turbines, solar photovoltaic (PV) arrays, and other renewable technologies such as geothermal generation, main grid connection/interconnection switch, and energy-storage devices such as flywheels and batteries for long and short term storage. The typical range of microgrid rating is 500 kW-15 MW.

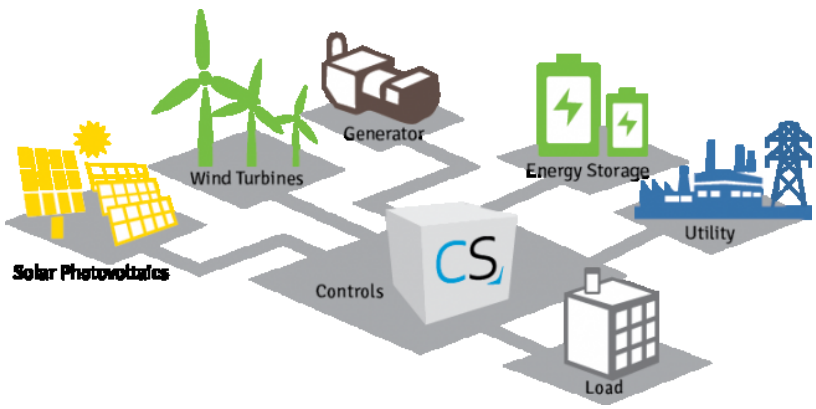

Fig. 2. Pictorial representation of a microgrid

The pictorial representation of the microgrid is shown in Fig. 2 which consists of photovoltaic system, wind turbines and fuel based generator as the distributed generation sources, while one control unit is also shown which is used to control the flow of power between utility grid,

microgrid and load. Battery in form of energy storage device is used for backup in case the microgrid islands.

1.2.2 MICROGRID TOPOLOGY

Microgrids can operate in parallel with the service grid or in the islanded mode during the faulty conditions or planned events. This type of distribution grid structure offers potential for improvement in power supply efficiency and reliability of power supply in comparison with the traditional and passive distribution grids. But the optimal topology for this kind of power distribution network is the well-known approaches which include a radial, a normally open-loop, or a meshed structure for the distribution systems. The possible network configurations of microgrid optimal topology are shown in Fig.3

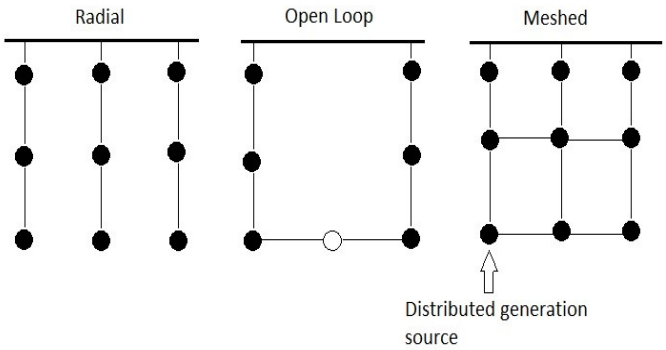

Fig. 3. Traditional distribution network topology [9]

Factors determining the selection of optimal microgrid network topology include [10]

- Size, type and location of microsources and loads.
- The power quality which a microgrid has to provide to the consumers also decides the optimal structure of the network.
- Economic resources available or the available budget.
- Cost of investment which includes the cost of primary equipments, protection, control equipments and communication technology.
- Operating and maintenance costs which might include cost of power losses during transmission and energy not supplied due to interruptions.

- Technical constraints which are protection system, voltage profile of the system and physical equipment dimensions.
- Voltage level of the system (medium-voltage networks are usually open-loop networks and low-voltage networks are radial, with normally open-loop topologies in some exceptional cases).

1.2.3 REASONS FOR INSTALLATION OF MICROGRIDS

Some of the various reasons for installation of microgrids are mentioned as follows

Limitation of fossil fuels: The reserves of the fossil fuels present in the environment are getting shorten day by day, it is just a matter of time that we exhaust all of our non renewable fuels. The dependency on fossil fuels have to be molded for the generation of power in order to keep our homes lighted in coming future hence the adoption of microgrid is one of the best alternative that one could realize up to now.

Less environmental pollution: The microgrid consists of the DG sources which are mostly based on renewable sources of energy, these DG systems do not consume the environmental fuels hence there is no problem of the production of exhausts which are polluting in nature. Usually in case of the thermal and nuclear power generation plants the byproducts are first treated before disposing them in to the environment, this kind of technology is not required in case of the renewable sources of generation.

Rising cost and burdens of transmission and distribution (T&D) infrastructure: The building of new transmission and distribution network has become a challenge nowadays because of the high cost of the materials and labors and also there are many other issues with the setting of T&D in remote areas which include land acquisition permissions and availability of skilled labor. Hence the microgrids in which generation is not far away from the load is useful.

Integration of renewable and storage technologies: The integration of the renewable energy sources and storage technologies have made the microgrid systems more efficient. One of the major concern with the microgrid is generation of enough power to serve the loads present in the system, the same issue can be overcome with the use of the storage technologies in which the new and improved storage devices are used having high efficiency. During the off load hours the

energy is stored in the storage devices and during the peak hours these devices provide the back up to the microgrid system. Moreover, the integration of renewable and advanced energy storage devices provide a stable and normal operation of the microgrid system. The voltage and frequency profile of the system can be improved using the energy storage techniques.

Power quality and reliability: The microgrids can operate in parallel with the utility grids hence the power quality is maintained at the consumer end even if the utility grid suffers from small system disturbances. The systems in which the microgrids operate in parallel with the utility grid are more reliable because during the faulty conditions on the main grid the microgrid can still operate to serve some part of the total load.

Public policy: The public policy has gone through a vast change from the past days. Today it favors distributed generation which offers improved efficiency, lower emission, enhanced power system security, better power quality and other benefits of national and international interests. Policies supporting this include tax credits, renewable portfolio standards, emission restrictions, grants and so on.

More knowledgeable Energy Users: Energy users are becoming more aware of alternative power approaches and are more willing to consider on site or distributed generation options than in the past. Many are interested in combined heat and power (CHP) as well as reliability enhancements.

1.2.4 CHALLENGES TO THE ADOPTION OF MICROGRID

Some of the technical challenges that must be overcome to achieve stable, economic and secure operation of microgrid which must deal with the following aspects.

Intermittent renewable generation: The microgrid consists of the distributed generation sources which could be a wind turbine, photovoltaic generator, small hydro systems etc. The electric power generated from all these sources largely depends upon the weather or climatic conditions, e.g. in case of wind turbine the turbine output depends upon the wind currents available, so the output level of the power generated from these microsources is not fixed hence

these are called as the intermittent renewable sources. These sources have limitations in any power system to provide a stable power level which is the basic requirement of any of the power network.

Low grid inertia: In a grid connected system the new renewable distributed generation sources and conventional generators operate together. The conventional generator includes diesel generators or synchronous generators while the distributed energy sources can have photovoltaic generators or wind turbine generators which are connected to ac grid by using some high grade converters, these DER's have low or no inertia and hence their integration with the service grid causes stability problems.

Coordination among distributed energy resources: Microgrids may have many types of distributed energy resources, such as diesel generator, microturbine, fuel cell, energy storage device, and so on. These DERs generally have different operating characteristics with respect to their generation capacity, startup and shutdown time, ramping rate, operation cost or efficiency, energy storage charging or discharging rate, and intertemporary control limitations. The operation of the microgrid must consider the operating characteristics of different components and optimal control strategies should be provided to ensure economic and secure operation.

1.3 NEED FOR CONTROL AND OPERATION

Microgrids are comprised of different components such as distributed generators, such as microturbines, fuel cells, PV generators, diesel generators etc, these components can be controlled in a continuous manner or in a discrete way in order to keep microgrid running in grid connected or islanded operating modes, as well as to guarantee a smooth transition between two modes. A major challenge related to microgrids is control and coordination of a variety of components in the microgrid to facilitate their parallel operations without loss of voltage and frequency stability, and doing so in most economic way. Control techniques and approaches have a wide divergence and that vary as per type of microgrid to achieve its best performance.

1.4 DISSERTATION PLANNING

Chapter 1 describes the problems arising with the conventional power generation sources and how the microgrids are helpful in providing a solution for the future and at the same time a glimpse of the work carried out is given. In Chapter 2, the literature survey of the control configuration of microgrid is discussed. The detailed description of the photovoltaic system, identification of gap in research and objectives of dissertation are also presented in the same chapter. In Chapter 3, the modeling of PV generator as a component of microgrid, description of the controller proposed control configuration of microgrid and simulation work is discussed. The simulation results are discussed in chapter 4. Finally, the conclusions and scope of future work are given in Chapter 5.

CHAPTER 2
LITERATURE REVIEW

The literature survey on single phase and three phase microgrid control configuration is carried out in this chapter. After that the photovoltaic system is described in detail which includes working of a single PV cell, then various module and array configuration to make a PV generator and its equivalent model etc. In addition, modification of the output of the PV cell with the changing weather conditions is also studied.

2.1 MICROGRID CONTROL CONFIGURATION

As the microgrid consists of microsources having their outputs uncertain hence there are many control schemes which can be used to control the power flow in a microgrid. For e.g. the PV and wind microgrid control is explained in [11] using a mathematical model, centralized supplementary controller to stabilize an islanded microgrid is given in [12], a virtual impedance optimization method for reactive power sharing in networked microgrid is explained in [13], similarly, there are many verified control schemes which are available in references[14-16]. The microgrid control configuration is modified in the dissertation work with a replacement which is discussed in the next chapter, before stepping on to the modification in the configuration the detailed description and working of the configuration is required which is accounted in this section first for the single phase [17] and afterwards for the three phase configuration[18].

The technique, proposed in [17], uses the capacitor current and its derivative in a control loop consisting of the PWM (Pulse width modulator) modulator so as to find the ON/OFF states of the switching devices present in the inverter. Although this control scheme/algorithm is successfully used in single phase and three phase inverters but it has some limitations as listed below

a) The scheme has a complex structure

b) Parameter variations may cause disturbance in algorithm

c) The load parameters need to be known first for the implementation of this control algorithm [19].

The control scheme has many advantages when used for UPS systems. It has two loops; inner loop is the current loop while the outer loop is the voltage loop which are as shown in Fig. 4. The inner loop provides a restrain to the increase in the peak current of the power circuit. While the outer loop checks the fluctuations in the load voltage, improves the dynamic response of the system and reduces the Total Harmonic Distortions (THD) in the load voltage.

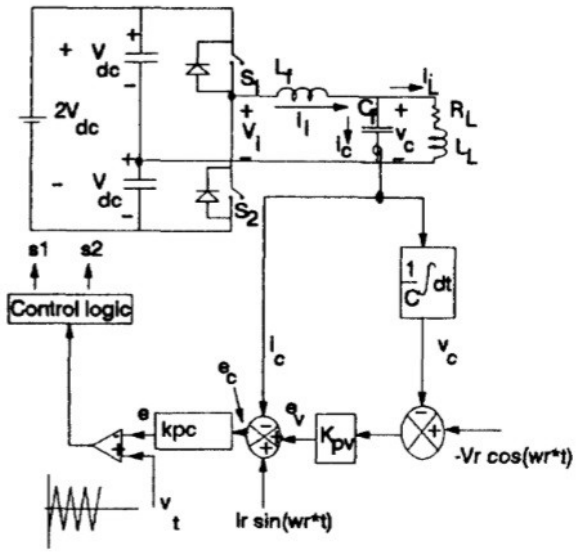

Fig. 4. Control Scheme of the single-phase UPS inverter [17]

The working of the control scheme is as follows, the outer capacitor voltage of the inverter filter is compared with the reference signal, the generated error $e_v(t)$ is passed through the proportional controller (K_{pv}) and then compared with the capacitor current of the inner loop. The final error $e_c(t)$ is then compared with the fixed frequency triangular signal after passing through another proportional controller (K_{pc}) in the current loop. The switching patters for the inverter switches are hence generated.

The control scheme having outer voltage and inner current loops used for the three phase UPS systems is as shown in Fig.5 [17] [18]. The three phase control scheme works in a similar manner as that of the single phase only the reference voltage waveform of the each phase are

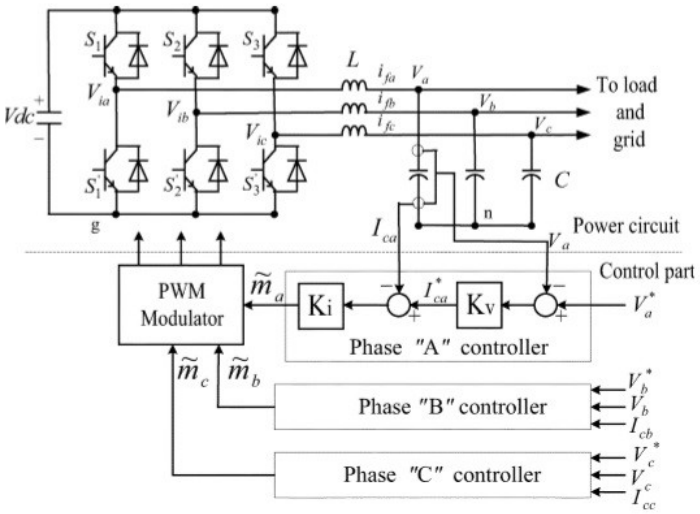

Fig. 5. Control scheme of the three-phase UPS inverter [8]

For phase 'a', the outer capacitor voltage v_{ca} is compared with the reference voltage of the inverter control circuit v_a^*, the error $e_v(t)$ is passed through the proportional controller of the voltage loop (K_v) so as to give the reference signal for the inner current loop. Now this new reference signal (I_{ca}^*) is then compared with the with the actual capacitor current of the inner current loop. The new generated error $e_c(t)$ is passed through the proportional controller of the inner loop and then is finally compared with the fixed frequency triangular signal so as to generate inverter switching pattern. The phase 'b' and 'c' controllers works exactly in the same manner the only difference is of the reference signal for each phase which is at 120 degrees phase difference.

2.2 CHOICE OF MICROSOURCE

The microsources may have many forms which are used in a distributed generation system some of the microsources are solar photovoltaic generators, small hydro systems, wind turbines, fuel cells, vehicle to grid systems etc. Although wind energy has dominated the renewable energy pool with a total of 23439.26 MW [20] of generation capacity in India but generation of energy

from the wind turbines is purely area specific hence this source may be the most successful way of harnessing energy from the renewables but it is not the most popular source of harnessing the renewable energy. The solar energy in which the photovoltaic cells are used to harness the solar energy is gaining the popularity day by day in commercial as well residential applications. In some of the states the government has made the use of solar system mandatory with the utility supply in case of commercial buildings. The photovoltaic systems can be installed easily on the rooftops and the new GPS (Global Positioning System) technology in which the solar array follows the position of the sun has made this system more efficient. The total installed capacity of solar systems in India is 7564.863 MW [21] but is expected to increase very fast in the coming future. The photovoltaic generators are hence considered as a microsource in the work carried out in this dissertation, the detailed explanation and working of a photovoltaic system is given in the next section.

2.3 PHOTOVOLTAIC SYSTEMS

2.3.1 BASIC WORKING PRINCIPLE [22]

To understand the working principal of a solar cell, let us consider one p-n junction diode be exposed to the sunlight. As according to the photon theory the solar light consists of packets of energy called as photons. When these photons are absorbed by the p-n junction diode the electron-hole pairs are formed in the diodes which are free to move, when these electron-hole pairs reaches the junction of diode the electric field of the depletion region pushes the holes to the p-side of the junction and electrons to the n-side of the junction. The p-side now has a majority of holes while the n-side has a majority of electrons which is shown in Fig.6. The p-n junction is now polarized and hence there is some voltage potential across it. If the connecting wires are connected across its p and n sides, the electrons flow from the n-side to the load, load to p-side of the diode as shown in Fig. 7. The holes are immobile ions hence the flow of electrons causes the flow of current. The electrons recombine with the holes on the p-side. By convention the direction of current is in the opposite direction to the flow of the electrons hence the current flows from p-side to n-side. An approximate equivalent circuit of solar cell is shown in Fig. 8 having a current source in parallel with the real diode.

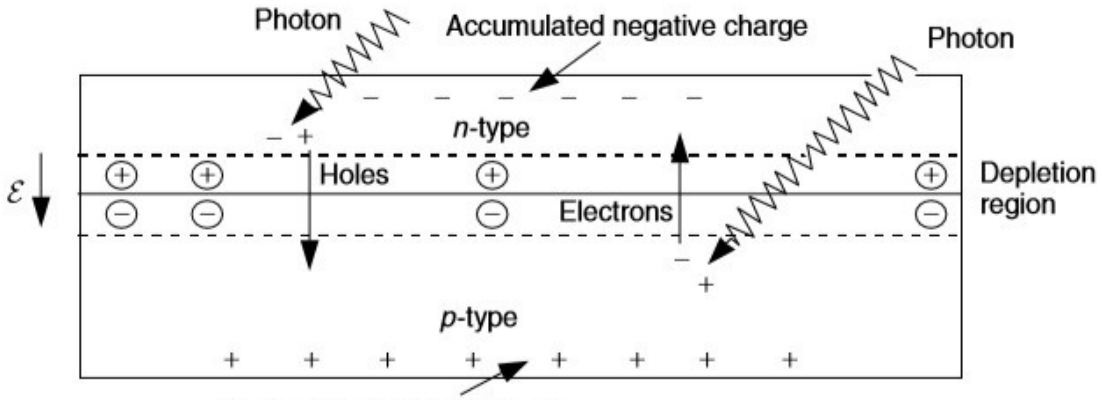

Fig. 6. Electronic model of photovoltaic cell [22]

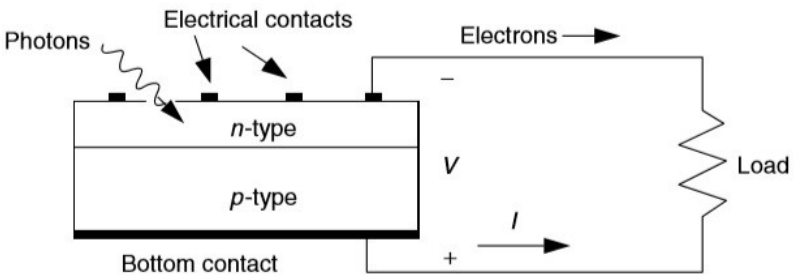

Fig. 7. A simple equivalent circuit of a PV cell [22]

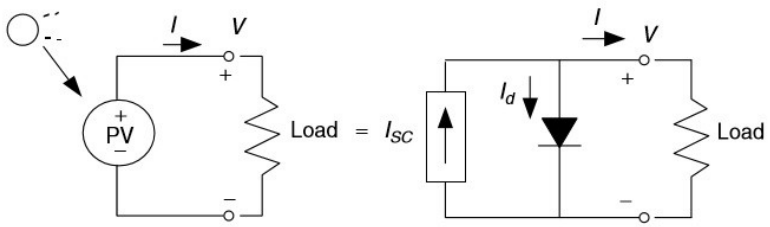

Fig. 8. A simple equivalent circuit of a PV cell [22]

2.3.2 DEPENDENCY OF I-V CURVES ON WEATHER CONDITIONS

2.3.2.1 AMBIENT TEMPERATURE AND SOLAR INSOLATION

The shift in the I –V (current-voltage) curves with the change in the ambient temperature and solar insolation for a typical solar cell is shown in Fig. 9. The change in the irradiance level causes the short circuit (I_{SC}) current to change in direct proportion i.e. the short circuit current of solar cell is directly proportional to the solar insolation level to which the cell is exposed. So if irradiance is reduced to ¼ of its previous level, the short circuit current will also reduce to ¼. The open circuit voltage of cell do not shows a significant change with irradiance because of its logarithmic relationship with short circuit current.

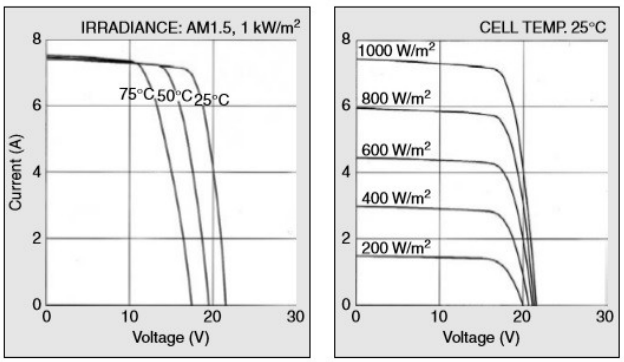

Fig. 9. I-V characteristic curves for Kyocera KC120-1 PV module under various cell temperatures and irradiance levels [22].

The ambient temperature has equally dominant effect on the I-V curves of the solar cell. For every one degree rise in the temperature the open circuit voltage falls by 0.37 % and the short circuit current increases by 0.05%. So it's not necessary that photovoltaics will perform better on the hot days. Fig. 9 illustrates both of these effects for a particular solar cell when various temperature and irradiance ranges are considered.

2.3.2.2 SHADING EFFECTS

To understand the shading phenomenon, let us consider Fig. 10 in which n cells are connected in series to form a module. Fig. 10 (a) is having n cells in sun while in Fig. 10 (b) the top most cell of the module is under complete shade.

When the n cells are in sun, all the cells present in the configuration contributes towards the output voltage of the module with voltage V while the same short circuit current I flows through them.

Now consider the case when the top most cell in the module is under the complete shading effect. The rest of the n-l cells still produce their original voltage of V_{n-1} and the same current I flows through them since the current remains same in series. Due to shading effect the current source of the shaded cell is deactivated and the module current I flows through the parallel and series resistance of that cell (R_P and R_S) because of the reverse biasing of the diode. This voltage drop across the resistances is opposite to the net module voltages and hence is subtracted from the net V_{n-1} voltage causing a further decrease in the net voltage of the module. Hence the shunt voltage V_{SH} of the module under shading can be expressed in equation (1)

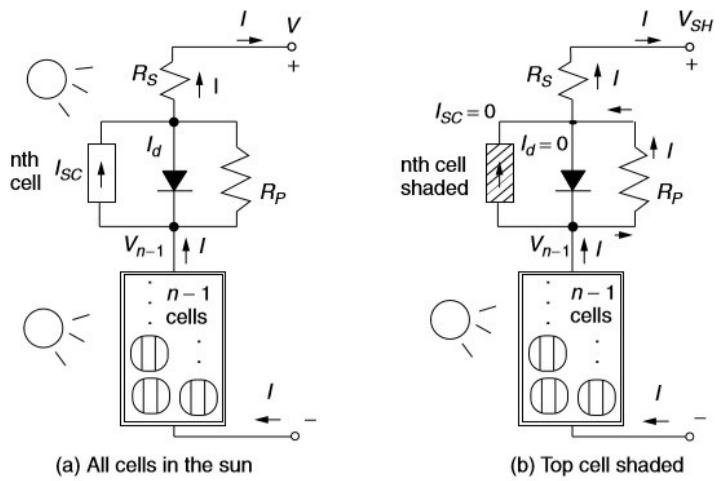

Fig. 10. A module with n cells in which the top cell is in the sun (a) or in the shade (b) [22].

$$V_{SH} = V_{n-1} - I(R_p + R_s) \quad (1)$$

The output voltage of the n-1 cells will be

$$V_{n-1} = \left(\frac{n-1}{n}\right) V \quad (2)$$

combining (1) and (2) gives

$$V_{SH} = \left(\frac{n-1}{n}\right)V - I(R_p + R_S) \quad (3)$$

The drop in the voltage ΔV at any given current I, caused by the shaded cell, is given by

$$\Delta V = V - V_{SH} = V - \left(1 - \frac{1}{n}\right)V + I(R_P + R_S) \quad (4)$$

$$\Delta V = \frac{V}{n} + I(R_P + R_S) \quad (5)$$

Since the parallel resistance R_P is so much greater than the series resistance R_S, (5) simplifies to

$$\Delta V \cong \frac{V}{n} + IR_P \quad (6)$$

2.3.3 EQUIVALENT MODEL OF A SOLAR CELL AND RELEVANT EQUATIONS

The simplest of equivalent circuit of a PV cell consists of a current source in parallel with the real diode (Current source delivers current in direct proportion to irradiance to which it is exposed). But a more practical circuit of a PV cell consists of series and parallel resistances [22] as illustrated in Fig. 11. The presence of series resistance (R_S) is due to resistance of the semiconductor while the parallel resistance (R_P) is the leakage resistance. Where I_0 is the reverse saturation current and V_d is the diode voltage.

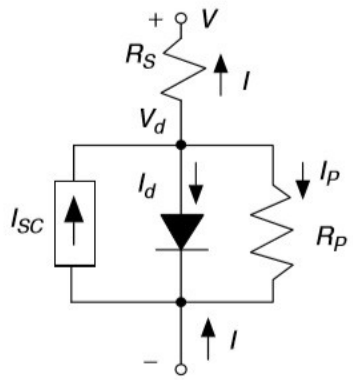

Fig. 11. Equivalent circuit of a PV cell [22]

$$I = I_{sc} - I_0\left(e^{38.9Vd} - 1\right) - V_d/R_p \quad (7)$$

$$V_d = 0.0257\ln\left(\frac{I_{sc}}{I_0} + 1\right) \quad (8)$$

$$V = V_d - IR_s \quad (9)$$

Solar Insolation Effect

As the solar insolation level decreases, short circuit current of the cell decreases in direct proportion as given in equation (10). So if we reduce the solar insolation to half of its previous level, the short circuit current (I_{SC}) is also reduced to half. Decreasing solar insolation also limits open circuit voltage (V_{OC}) of the cell, but the V_{OC} has a logarithmic relationship with I_{SC} that results in relatively modest changes in V_{OC}.

$$I_{SC} \propto \text{Solar Insolation} \tag{10}$$

Temperature Effect

The change in the ambient temperature has a significant effect on the open circuit voltage (V_{OC}) of the PV cell while the variation on the short circuit current (I_{SC}) with the temperature is very nominal. For every one degree rise in the temperature the V_{OC} drops by 0.37 % and I_{SC} increase by 0.05%. PV systems can perform better if the temperature is not much high.

$$V_{OC} = V_{in}[1 - 0.0037(T_{am} - T_{st})] \tag{11}$$

$$I_{SC} = I_{in}[1 + 0.0005(T_{am} - T_{st})] \tag{12}$$

Where V_{in} and I_{in} are the open circuit voltage and short circuit current of the cell at the standard temperature (Tst) i.e. 25 ^{o}C. Whereas T_{am} is the ambient temperature.

Shading Effect

The output voltage of a PV module can reduce significantly even if a small portion of the module is shaded. If we have a string of n cells connected in series to form a module and one cell gets shaded then the output voltages produced by that cell will be zero plus the voltages drop across the series and parallel resistances of that cell will be subtracted from the total output voltages of the module. Hence, the total voltage of the module is given by following equation (13)

$$V = n(V_d - IR_s) \tag{13}$$

Now change in the voltage after one cell gets shaded will be

$$\Delta V \cong \frac{V}{n} + IR_p \quad (14)$$

The equivalent model of the PV cell is designed in the Simulink in MATLAB (R2014a) by utilizing the equations (7-14).

2.3.4 FORMATION OF SOLAR MODULES AND ARRAYS

The individual single PV cell can produce only about 0.5 Volts, so it is very rare to use the single solar cell in any application. Instead the PV cells are connected in series to form a module and all the cells are encased in tough, weather resistant packages. The most commonly used module is the '12 V module' in which the 36 cells are connected in series such that the voltage contribution of each of the cell adds up. The 12 V module is most commonly used in many applications, one such application is the simple battery charging systems. The series connection of the solar cells can result in many such modules for e.g. if the 72 cells are connected in series then '24 V module' can be obtained, so the voltage requirement of any application can be justified. However a module with higher voltage level can be operated to made at lower voltage level by field wiring i.e. 24 V module can act as 12 V module. The modules can be further connected in series to increase the voltage levels and also these modules can be connected in parallel to increase the current requirements, this series and parallel combination of modules is known as the solar array.. Fig. 12 shows the distinction between a cell, module and an array.

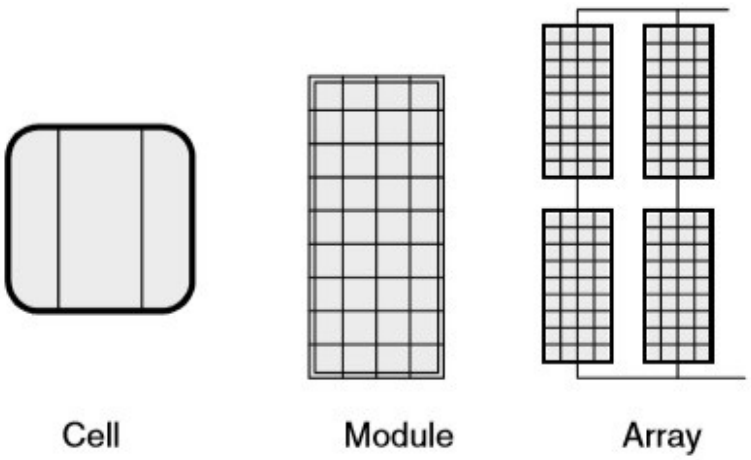

Fig. 12. Photovoltaic Cell, Modules, Array

FROM CELLS TO MODULES

When Photovoltaic cells are connected in series, they all carry the same current, and at any given current their voltages add as shown in Fig. 13. The net voltage across the module can be calculated by multiplying the voltage across each cell with the total number of cells in the module.

$$V_{Module} = n(V_d - R_S) \quad (15)$$

FROM MODULES TO ARRAYS

PV modules can be connected in series to increase voltage or in parallel to increase the current, this series and parallel combination of the modules make up an array. Considering the typical design, it is very important to know the approximate current and voltage of the load before designing a particular PV array. When connected in series, the module I-V curves just add up on the voltage axis, which is shown in Fig. 14. For the cells connected in parallel, the current of each module adds up and hence the current axis of the I-V curves adds up as in Fig. 15, in which three modules are connected in parallel. The series and parallel combinations largely depends upon the power required from the PV array.

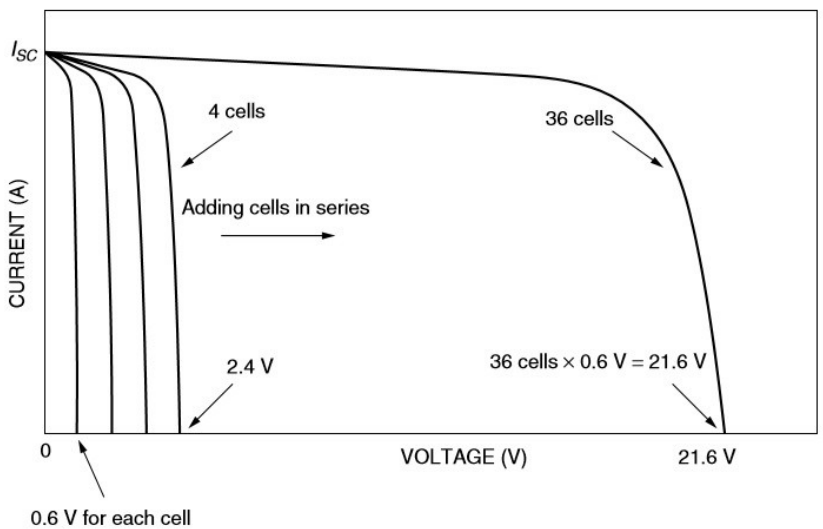

Fig. 13. I-V curve for a module having 36 cells [22].

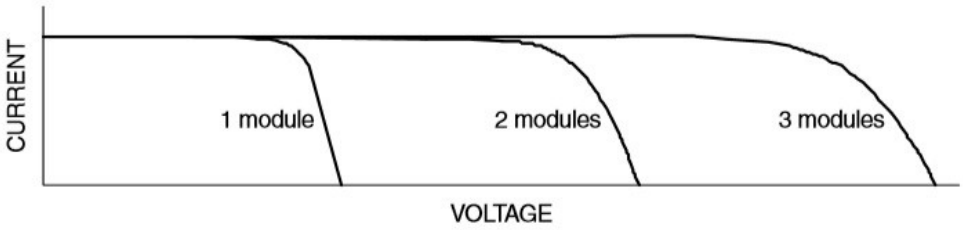

Fig. 14. Modules in series

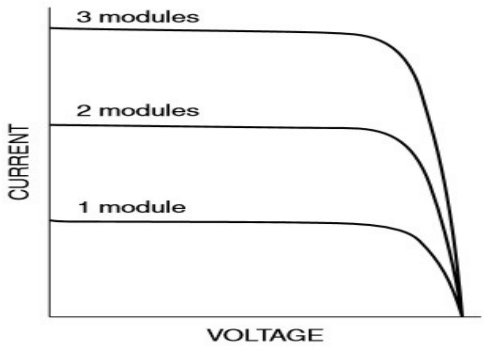

Fig. 15. Modules in parallel

2.4 IDENTIFICATION OF GAP IN RESEARCH

The detailed description of the control configuration of the microgrid is already accounted in the section 2.1 of this chapter. The configuration employs PWM (pulse width modulation) scheme and responds very well to the change in the reference voltages and hence changes its output according to the change in the reference voltage of the inverter controller. The values of the gain of the proportional controllers are configured as according to their frequency responses. This particular microgrid configuration is used in many applications like synchronizing two microgrids, synchronizing a microgrid and a utility grid, active and reactive power control etc. But under many application of this control configuration the microsource is represented as a fixed dc source, which is not valid for many microsources. In many applications of the above control configuration, the shift in the voltage/current levels of the microsource with time and change in weather conditions is neglected as fixed dc source is considered to represent the microsource in which the voltage and current levels remains constant. In our study the microsource is considered as the photovoltaic generator, a detailed analysis on how the voltage and current level of the PV generator change with the weather conditions is already made in

section 2.3.2 of this chapter. The PV generator is replaced as the fixed dc source and various observations are made, further the improvement of the response of the configuration with the replacement is further carried out which is discussed in the next chapters.

2.5 OBJECTIVE OF DISSERTATION

Based on the literature survey presented in the previous sections and identification of gaps in research, the following objectives of present dissertation work are proposed.

a) Modelling and simulation of the photovoltaic generator whose output depends upon the weather conditions i.e. solar insolation to which the same is exposed, ambient temperature and number of shaded cells in a PV generator by using the Simulink in MATLAB 2014.
b) To propose a control configuration of the microgrid considering properly modelled photovoltaic generator as a microsource instead of representing the same as fixed dc source.
c) Performance analysis of the proposed controller for the microgrid configuration based on active and reactive power response of the microgrid in islanded mode using droop characteristics

CHAPTER 3

MICROGRID WITH PV GENERATOR AS MICROSOURCE

3.1 INTRODUCTION

The control configuration of the microgrid as explained before is modified with the replacement of fixed dc source with the PV generator in single phase and as well as for the three phase configuration of the microgrid. The replacement ensures a more practical operation of the microgrid. The output level of the generator now depends upon the solar insolation to which the generator is exposed, ambient temperature and number of shaded cells in module [22]. For the purpose of simulating the microgrid model under varying weather conditions the sample solar and irradiance data of Patiala for the month of April is considered [23], which is collected from the weather station at Thapar University, Patiala. The microgrid model is simulated under the sample data both for the single phase and as well as for the three phase configuration and various outcomes are recorded using Simulink. The frequency response analysis of the configuration with fixed dc source and with PV generator as microsource is also carried out to distinguish clearly between two configurations. The controller based on the droop characteristics are first described and are then used in the new microgrid configuration to uplift the active and reactive power levels in the microgrid under islanded mode. The new results are hence obtained by simulating the microgrid configuration with the newly designed active and reactive power controllers. All the results are obtained and verified using the simulations in Simulink MATLAB software.

3.2 CONFIGURATION OF MICROGRID

The configuration of the microgrid is shown in the Fig. 16 in which the two parallel DG systems 1 and 2 are used. Each DG system consists of one PV generator (acting as the dc voltage source) whose dc voltage level depends upon various weather conditions, a pulse-width modulation (PWM) voltage source inverter and LC filters. The microgrid is assumed to be working in the islanded mode.

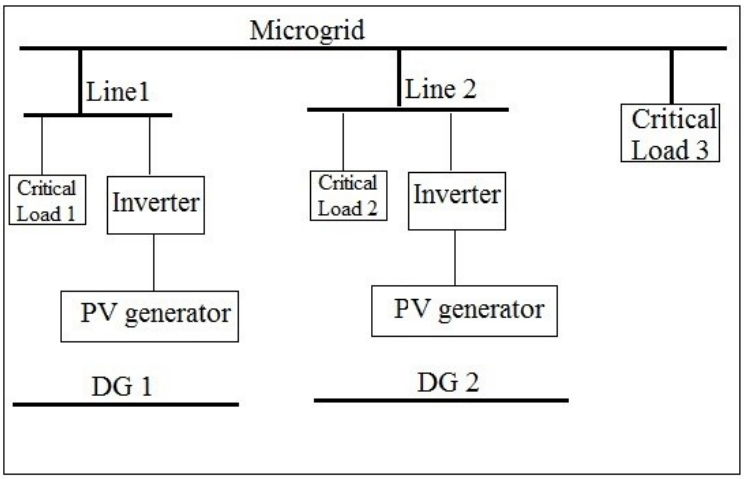

Fig. 16. Microgrid configuration

Three loads are considered in the microgrid configuration, which can be single phase or three phase. For single phase and three phase analysis the above given configuration remains same but only the type of inverter and nature of load change as per single phase or three phase configuration.

3.3 MODELLING OF PV GENERATOR

The photovoltaic cell/generator is designed by utilizing the equations (7-14) which are described in section 2.3.3. The above equations include the effects of changing weather conditions around the PV generator. Those equations are coded in the user defined MATLAB function in Simulink. The coding is done by considering the irradiance level, ambient temperature and number of shaded cells as the input while voltage level and current level of the cell are output.

The coding used to create a photovoltaic generator in a MATLAB function is as given below, V_{OC} and I_{OUT} are the output voltage and current of the PV generator. The three inputs are the solar insolation of the sample data (Ins), ambient temperature input of the sample data (T) and the number of shaded cells in an array (m). The rest of the variables considered are explained in the coding itself.

```
function [Voc,Iout]= fcn(Ins,T,m)
%#codegen
Rs=0.005; % Series resistance
Rp=6.6; % Parallel resistance
Io=((10^-10)); % Reverse saturation current
```

```
Vd=0.5; % diode junction voltage
n=25; % no of cells in series in a module
ns=25; % no of modules in series in an array
np=20 ; % no of modules in parallel in an array

% Irradiance effect
Isc1=4; % at Ins=1000
Isc2=(Ins/1000)*Isc1;
Isc=Isc2*(1+ (0.0005*(T-25)));
Id=Io*(exp(38.9*Vd)-1);
I=(Isc-Id-(Vd/Rp));
Iout=np*I;
Voc1=ns*n*(Vd-(I*Rs));

% Temperature effect
Voc2=Voc1*(1-(0.0037*(T-25)));
Voc3=Voc2;

% Shading effects
dV=m*((Voc3/(n+ns))+(I*Rp));
Voc= Voc3-dV;
```

The designing of the module from one cell and array from module is as explained here.

1 CELL : 0.4805 Volts (Under 'STC')

3.896 Amperes (Under 'STC')

1 MODULE : 25 cells are connected in series to deliver

25×0.4805= 12 Volts

3.896 Amperes

1 ARRAY : the modules can be connected in series to fulfill the voltage requirements and can be connected in parallel to increase the current levels. The arrangement of modules in an array is different for three phase and single phase configurations and hence are arranged according to voltage and current levels.

The solar insolation and temperature data of Patiala is considered which is input to the previous function, the data is considered. The hourly data is considered hence the code is generated by utilizing the clock in the user defined function.

SOLAR INSOLATION

The solar insolation input ('Ins') is as coded below. 't' is the input of the clock while 'u' is the variable with the numeric value of 1. The average solar insolation value for the first hour is 474.1953 W/m^2 and 647.55 W/m^2 for the next hour similarly the eight hour data is considered in the coding as input of the PV cell.

```
function y = fcn(u,t)
%#codegen
if t>=0 && t<=1
y = 474.1953*u;
else
    if t>1 && t<=2
        y = 647.55*u;
else
    if t>2 && t<=3
        y = 777.09*u;
else
    if t>3 && t<=4
        y = 819.93*u;
else
    if t>4 && t<=5
        y = 804.40*u;
else
    if t>5 && t<=6
        y = 719.65*u;
else
    if t>6 && t<=7
        y = 536.36*u;
else
    if t>7 && t<=8
        y = 321.88*u;
    else
        y=0;
    end
    end
    end
    end
    end
    end
    end
end
```

AMBIENT TEMPERATURE

The ambient temperature ('T') data which is the second input is as coded below having the average value of 34.25^{o}C in the first hour, 38.75^{o}C in the second hour and so on.

```
function y = fcn(u,t)
%#codegen
if t>=0 && t<=1
y = 34.25*u;
else
    if t>1 && t<=2
        y = 38.75*u;
else
    if t>2 && t<=3
        y = 41*u;
else
```

```
    if t>3 && t<=4
        y = 42.6*u;
else
    if t>4 && t<=5
        y = 43.6*u;
else
    if t>5 && t<=6
        y = 44*u;
else
    if t>6 && t<=7
        y = 43*u;
else
    if t>7 && t<=8
        y = 42*u;
    else
        y=0;
    end
    end
    end
    end
    end
```

3.4 MATHEMATICAL ANALYSIS OF MICROGRID CONFIGURATION

Consider the circuit diagram of single phase full bridge voltage source inverter (VSI) as shown in fig. 17 which is used in the control configuration of the microgrid. It is consisting of PV generator, filter (L_F and C_F), switches (S_1 to S_4) and an R-L load.

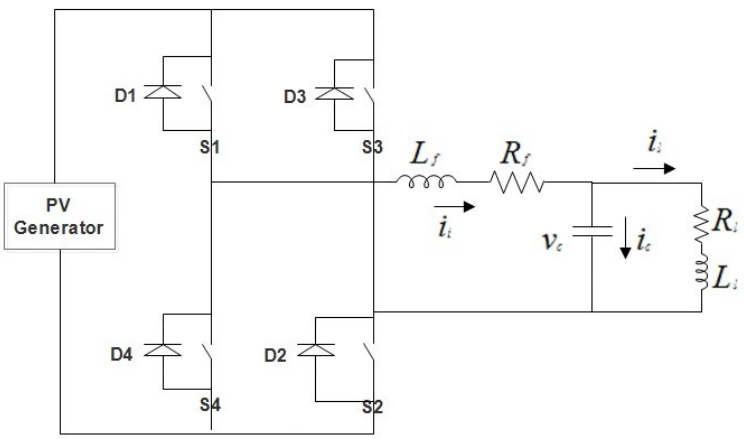

Fig. 17. Single phase full bridge inverter

Let us initially assume the output of the PV generator to be fixed as V_{dc} in order to make the analysis. The system differential equation can be written in the state space form as given in equation (16) which is obtained from [17].

$$d/dt\begin{bmatrix} i_i(t) \\ i_l(t) \\ v_c(t) \end{bmatrix} = \begin{bmatrix} -\frac{Rf}{Lf} & 0 & -\frac{1}{Lf} \\ 0 & \frac{Rl}{Ll} & \frac{1}{Ll} \\ \frac{1}{Cf} & -\frac{1}{Cf} & 0 \end{bmatrix}\begin{bmatrix} i_i(t) \\ i_l(t) \\ v_c(t) \end{bmatrix} + \begin{bmatrix} V_{dc}(2S_1^* - 1)/L_f \\ 0 \\ 0 \end{bmatrix} \quad (16)$$

Where $S_1^* = 1$ when both the S_1 and S_2 are ON and $S_1^* = 0$ when S_1 or S_2 is OFF. Equation (16) is discontinuous due to the presence of the switching function S_1^* so the averaged time-continuous model of the system is obtained by assuming inverter switching frequency, f_S, which is much higher than the frequency of the modulating signal $v_m(t)$. Hence the discontinuous switching function S_1^* is replaced by time-dependent duty cycle $d_1(t)$ [24].

$$d_1(t) = \frac{1}{2}\left(\frac{v_m(t)}{v_t} + 1\right) \quad (17)$$

where v_t is the amplitude of the carrier waveform. For a modulating signal given by

$$v_m(t) = V_m \sin(\omega_m(t)) \quad (18)$$

the system state-space averaged continuous equation can be obtained by substituting the discontinuous switching function, S_1^* in (16) by its averaged value in (17) and (18). The resultant system equation is obtained as

$$d/dt\begin{bmatrix} i_i(t) \\ i_l(t) \\ v_c(t) \end{bmatrix} = \begin{bmatrix} -\frac{Rf}{Lf} & 0 & -\frac{1}{Lf} \\ 0 & \frac{Rl}{Ll} & \frac{1}{Ll} \\ \frac{1}{Cf} & -\frac{1}{Cf} & 0 \end{bmatrix}\begin{bmatrix} i_i(t) \\ i_l(t) \\ v_c(t) \end{bmatrix} + \begin{bmatrix} MV_{dc} sin(\omega_m t)/L_f \\ 0 \\ 0 \end{bmatrix} \quad (19)$$

where M is the modulation index, defined as

$$M = \frac{V_m}{V_t} \quad (20)$$

The first row of (19) indicated that the averaging process replaces the effect of the inverter switching function with a controllable sinusoidal voltage source of magnitude MV_{dc}. Assuming the resistance associated with the filter inductor is negligibly small, the equivalent circuit of the averaged inverter system is as shown in Fig. 18.

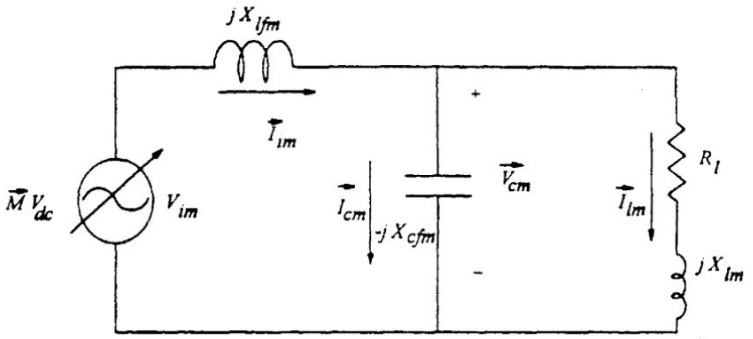

Fig. 18. Equivalent circuit of averaged Inverter system [17]

From the above equivalent circuit and the phasor analysis the inverter output voltages are given as

$$\overrightarrow{v_{cm}} = v_{dc}\,\overrightarrow{KM} \tag{21}$$

Where $\vec{M}$ is the phasor representation of the modulating signal $M\sin(\omega_m t)$ while the phasor $\vec{K}$ is given as

$$\vec{K} = \frac{X_{lm} - X_{cfm} - jR_l X_{cfm}}{X_{lm} X_{cfm} + X_{lfm}(X_{cfm} - X_{lm}) + j(R_l X_{lfm} - R_l X_{cfm})} \tag{22}$$

The equation (21) clearly shows the variation of the inverter output voltages ($\overrightarrow{v_{cm}}$) with the change in the v_{dc} when all the other components in the inverter are kept as fixed. The V_{dc} is assumed to be fixed as earlier just to carry out the analysis but it varies with the weather conditions as illustrated earlier.

3.5 VARIATION IN FREQUENCY RESPONSE OF THE INVERTER CONTROL

In this section the variation in the frequency response with the change in the source dc voltages of the closed loop voltage transfer function of the control scheme is investigated and various conclusions are further drawn. Let us first discuss in brief about the bode plot.

BODE PLOT [25]

Before moving on to the investigation of the frequency response of the control scheme it is necessary to discuss in brief about the information that we can gather from the bode plot of the various transfer functions. The Bode plot method gives a graphical procedure for determining the

stability of a control system based on sinusoidal frequency response. The variation of the magnitude of sinusoidal transfer function expressed in decibel and the corresponding phase angle in degrees being plotted with respect to frequency on a logarithmic scale in rectangular axis. The plot thus obtained is known as the Bode plot. Relative stability of a closed loop control system can be conveniently assessed by plotting its open loop transfer function by Bode plot method. The gain margin and phase margin is determined directly from the Bode plot.

The inner current-regulated voltage-controlled strategy used for controlling the single-phase grid interfacing VSI is shown in Fig. 19.

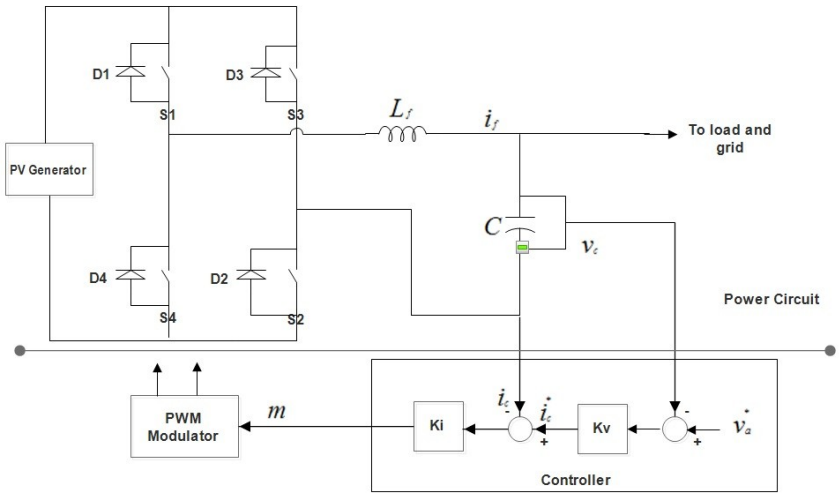

Fig. 19. Power circuit and control schematic for single phase inverter with LC filter [8] [17].

To develop the transfer function, the governing equations of the inverter are first written from [8] as

$$L_f \frac{di_f}{dt} = \frac{1}{2}\tilde{m}v_{dc} - v_c \quad (23)$$

$$C\frac{dv_c}{dt} = i_f - i_{load} \quad (24)$$

Where $\tilde{m} = mcos(\omega t - \varphi)$ is the modulating signal, C is the filter capacitor, v_c is the capacitor voltage, v_{dc} is the voltage generated by PV module (variable) and i_f,i_c and i_{load} are the currents flowing through filter inductor, capacitor and load respectively. The Laplace transforms of the equation (23), (24) gives us the inner current control loop transfer function. Once the inner current loop design is finished, the next step is to fine-tune the gain of the outer voltage feedback

loop, whose open-loop transfer function without considering the influence of load disturbance is given by

$$G_v(s) = \frac{v_c}{i_c^*} = \frac{i_c}{Cs\, i_c^*} \tag{25}$$

the performance of the capacitor voltage loop can be further improved by including an additional feed forward path for I_C^* as shown in Fig. 20. The transfer function of this feed forward path can be written as $I_C^* = V_C^* Cs$, and can conveniently be implemented by adding a differentiator block Cs to process the reference voltage V_C^*.

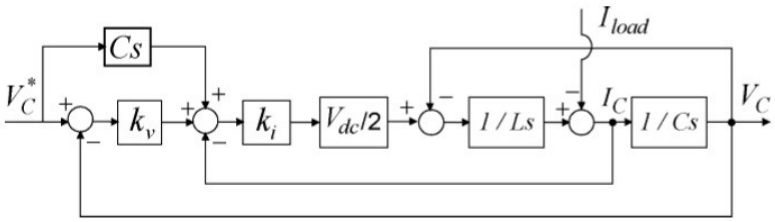

Fig. 20. Block diagram of the voltage and current loops with feed forward control.

With this feed forward path, the closed-loop transfer function of the outer loop can be written as

$$v_c = \frac{\frac{v_{dc} k_i}{2}(Cs + k_v)}{LCs^2 + \frac{v_{dc} k_i}{2}Cs + \frac{v_{dc} k_i k_v}{2} + 1} v_c^* - \frac{Ls}{LCs^2 + \frac{v_{dc} k_i}{2}Cs + \frac{v_{dc} k_i k_v}{2} + 1} i_{load} \tag{26}$$

K_V and K_I are the gains of the proportional compensator which are chosen as 4 and 1 respectively and L and C used are 3 mF, 150 μC.

Consider the eight hour solar insolation and temperature data for the month of April for the Patiala, India region as given in table I

Table I
SOLAR INSOLATION AND TEMPERATURE DATA [23]

Time Division	Hours	Solar Insolation (W/m^2)	Temperature (^oC)
0-1	9-10	474.1953	34.25
1-2	10-11	647.55	38.75
2-3	11-12	777.09	41
3-4	12-1	819.93	42.6
4-5	1-2	804.40	43.6
5-6	2-3	719.65	44
6-7	3-4	536.36	43
7-8	4-5	321.88	42

As the v_{dc} is not fixed it will be different for the different hours and the values of v_{dc} for these hours can be calculated by using the equations (7-14). The bode plots of V_c/V_c^* and V_c/I_{load} for the standard PV module working conditions i.e. 1000 W/m^2 solar insolation, 25^{o}C temperature and zero cells shaded in a module and with the average of the practical solar insolation and temperature data considered in table I i.e. 637.6319 W/m^2 solar insolation and 41.15^{o}C temperature with zero cells shaded are shown in Fig.21 and Fig.22 respectively, while the PV generator is considered to have dc voltage level of 300V.

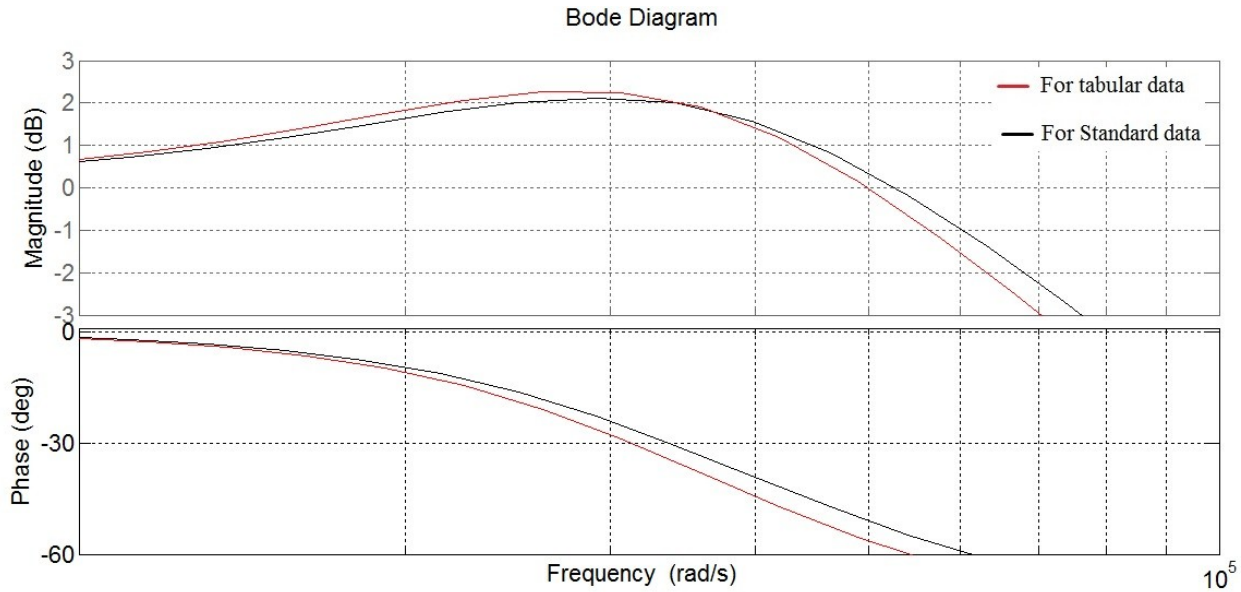

Fig. 21. Bode plot of V_C/V_C^* for different v_{dc}

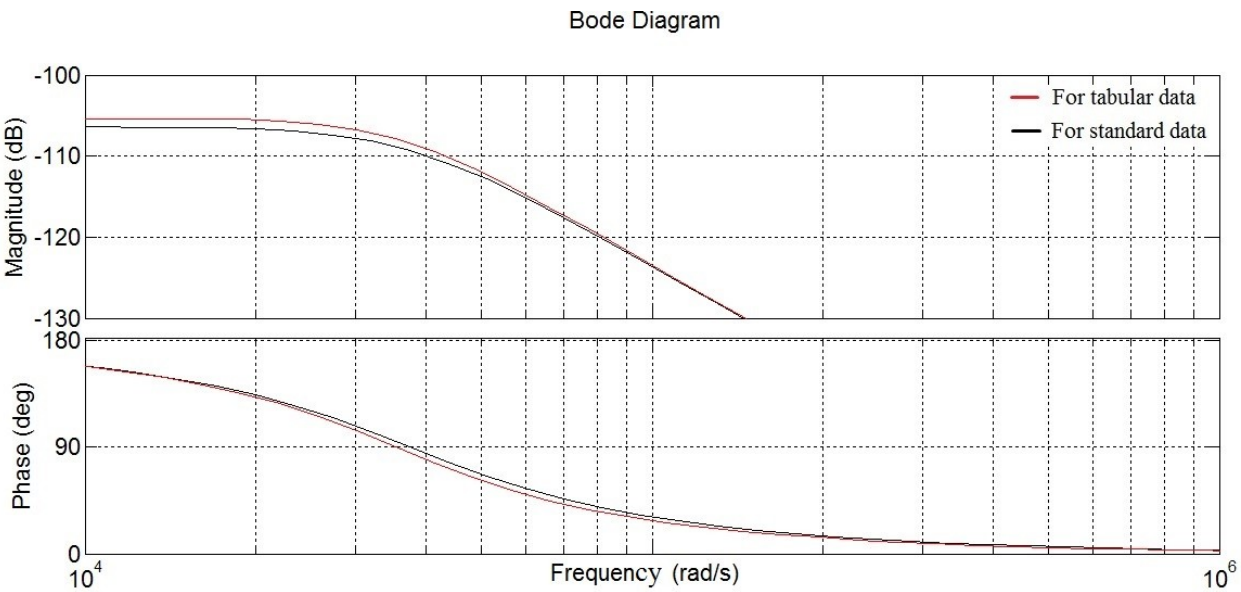

Fig. 22. Bode plot of V_C/I_{Load} for different v_{dc}

A close observation of the above two figures reveals that the control bandwidth is getting reduced when the PV module is operating under the data mentioned in table I as compared to when it is operating under standard working conditions. The gain margin for bode plot of V_c/I_{load} is also getting reduced from 2.0900e+05 to 1.8700e+05 and phase margin for the bode plot of V_c/V_c^* is shifting from 126.38 to 123.77 when the tabular data is considered for the PV generator.

3.6 ROLE OF THE CONTROLLER

There are several control approaches applicable to microgrids, they vary between fully decentralized and fully centralized approaches. In our microgrid system, a centralized controller is used for both the DG systems. The controller consists of further two sub parts i.e. active power controller and reactive power controller, the active power controller dictates the new reference voltage magnitude while the reactive power controller dictated the frequency and phase angle of the new reference voltages which is then applied to the inverter controllers of the DG system. Both the controllers are aimed at regulating the power fluctuations across the loads in the microgrid during the changing operating conditions of the microsource.

3.7 MICROGRID MODEL WITHOUT CONTROLLER

The microgrid simulation model without controller both for the single phase and for the three phase configuration is described in this section. Both the simulation models are simulated under the solar data provided in Table I and the results are presented separately in the results section.

3.7.1 SINGLE PHASE MICROGRID MODEL

The simulation model shown in Fig. 23 is simulated without the presence of the controller. The fixed dc source is replaced by the PV generator in the control configuration of the microgrid. The Simulink model is designed keeping in view that the microgrid is operating under the islanded mode hence the grid is not considered in the model.

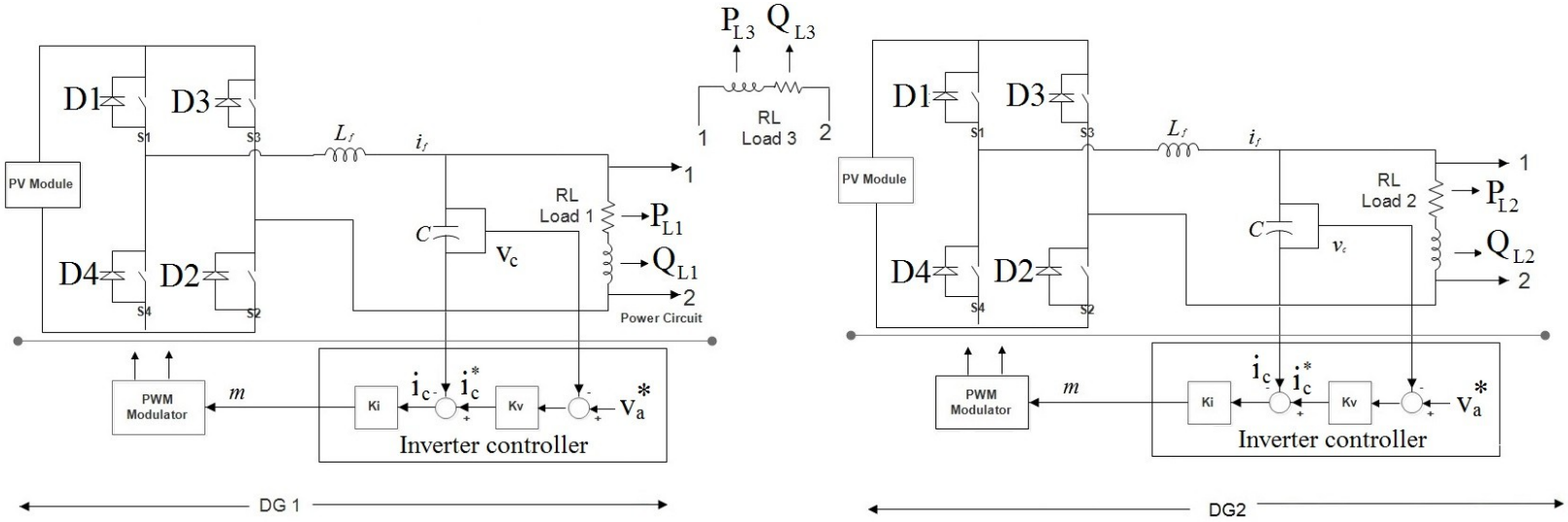

Fig. 23. Schematic representation of single phase simulation model without controller

The switches shown in the schematic diagram are actually the IGBT's which are used in actual simulation model, the sign block and the saturation block with the upper limit as 1 and lower limit as 0 is used to produce the appropriate switching signals for the switching devices under the PWM Modulator, the triangle generator is also used with a gain block so as to set the modulation index of the PWM scheme. The PV generator consists of an array having 25 modules in series and 13 modules in parallel so as to reach the voltage level of 300 Volts for this particular configuration. The PV generators are simulated using the data given in Table I. P_{L1},P_{L2},P_{L3} are the active power dissipation across the load 1,2 and 3 similarly Q_{L1},Q_{L2},Q_{L3} are the reactive power dissipation across the load 1,2 and 3. The inverter control parameters (K_i and K_v) are considered as according to the previous control configuration [8]. The reference voltage v^* is set at 230V since there is no feedback control. The values of the loads, filter inductor and capacitances used are given in Table II.

3.7.2 THREE PHASE MICROGRID MODEL

The schematic representation of the three phase microgrid simulation model without controller is shown in Fig. 24. The PV generators are again simulated using the sample data given in Table I while PV generator consists of an array having 59 modules in series and 13 modules in parallel so as to reach the voltage level of 700 Volts for the three phase configuration. The three phase microgrid model is almost same as that of the single phase model, the noticeable difference is that the three phase inverter is used and the inverter controller part has three controllers one for each phase. The controllers for phase "b" and "c" work in the same manner except that their respective reference waveforms are shifted from each other by 120 degree. The reference voltage v^* of each phase controller is again set at 230 V without feedback control. The detailed description of the system parameters is given in Table III.

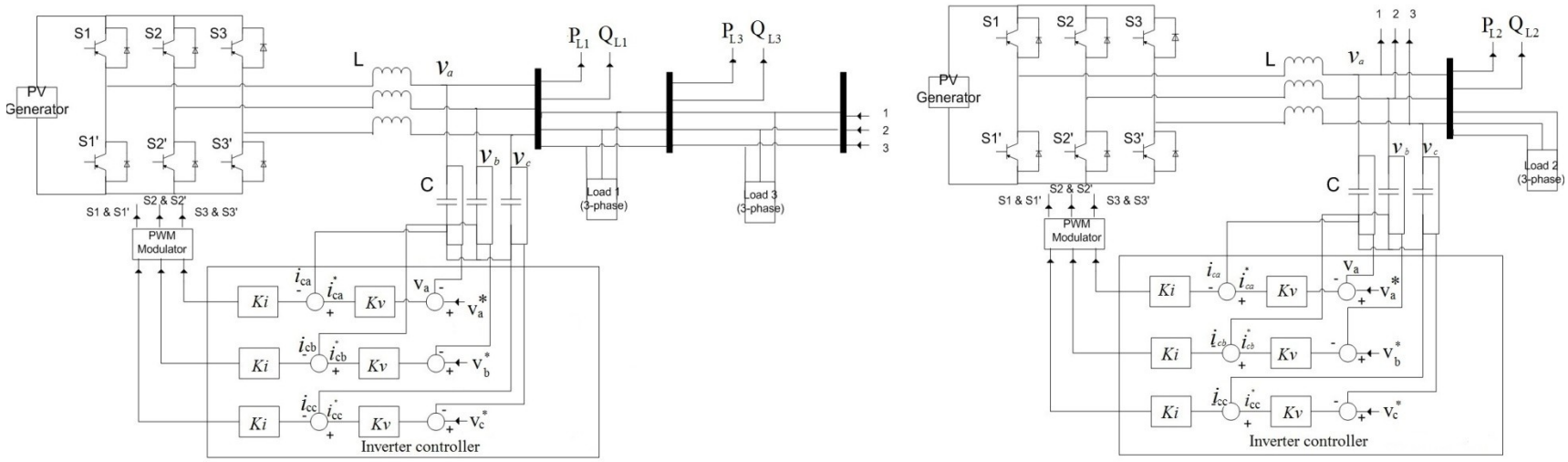

Fig. 24. Schematic representation of three phase simulation model without controller

3.8 CONTROLLER DESIGN

The design of the controller is based on the droop characteristics of P-ω (active power-angular frequency) and Q-E (reactive power-voltage magnitude) power loops [8]. The flow of the active power P between two nodes can be controlled by varying the supply frequency, while the flow of reactive power Q can be controlled by changing the voltage magnitude. Consider the P-ω droop characteristics as shown in Fig. 25.

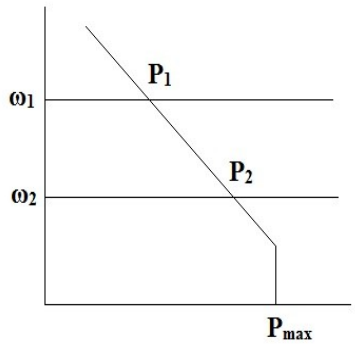

Fig. 25. P-ω droop characteristics

This droop characteristics mathematically be expressed as

$$\omega_2 = \omega_1 - \beta(P_1 - P_2) \quad (27)$$

$$\beta = \frac{\omega_1 - \omega_2}{P_1 - P_2} \quad (28)$$

P_1 is the active power across three loads under islanded mode and when PV generator operates under conditions given in table I. P_2 is the power across loads under grid connected mode of operation. ω_2 is the reduced frequency at which the required active power is consumed by the load. The Laplace transformation of the equation (27) and (28) is the basic guideline for designing active power controller as shown if Fig. 26

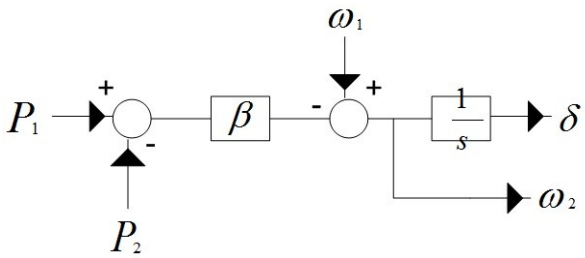

Fig. 26. Active power controller

The gain β of the controller is found using the equation (28), since the values of ω_2 and P_2 are uncertain. Hence minimum allowable operating frequency (ω_{min}) and maximum real power

(P_{max}) are used. The value of gain can be adjusted around the numerically computed value according to the operating condition dictated. In the similar manner, by utilizing the reactive power droop characteristics the reactive power controller can be designed. Considering the mathematical representation of the Q-E droop characteristics the following equation (29) and (30) are referred

$$E_2 = E_1 + \zeta(Q_2 - Q_1) \tag{29}$$

$$\zeta = \frac{E_2 - E_1}{Q_2 - Q_1} \tag{30}$$

Q_1 is the reactive power across loads under given operating condition of PV generator while Q_2 is the reactive power across loads under grid connected mode of operation of microgrid. E_2 is the voltage required to achieve required reactive power. For finding the gain (ζ) of the controller E_2 is replaced by E_{max} (Maximum allowable voltage) and Q_2 is replaced by Q_{max} (Maximum reactive power of system). The block diagram realization of equations (29) and (30) is shown in Fig. 27.

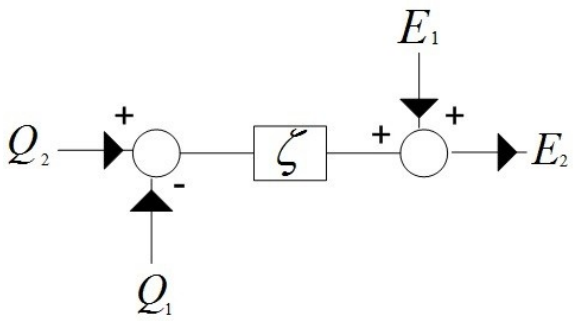

Fig. 27. Reactive power controller

The overall configuration of the controller is shown in Fig. 28. The output of the controller (v^*) is the new reference voltage for the inverter controller

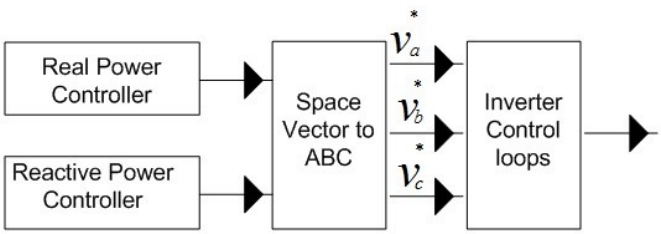

Fig. 28. Overall configuration of controller

3.9 PROPOSED MICROGRID MODEL WITH CONTROLLER

The controller described in the above section is used in the simulation models of the microgrid so as to match the active and reactive power levels when the PV generator operates under the varying weather conditions. The detailed description of the controller in single and three phase models is as given below and the improved results are presented separately in result section.

3.9.1 SINGLE PHASE MICROGRID MODEL WITH CONTROLLER

The simulation model with the controller is shown in Fig. 29. P_2 and Q_2 which are reference values to the controllers are obtained by simulating the microgrid model under standard operating condition of the PV generator. P_1 and Q_1 are the sum of the active and reactive power across the three loads present in the microgrid system. The sample and hold block used at the input of the controllers is programmed to sample the values of P_1 and Q_1 for some fraction of the hour and holds that value for the rest of the hour. The sample and hold block used at the output of the controller is programmed for proper coordination between input and output blocks. It means that while the output is being sampled, the input signal is put in hold condition and vice versa. It holds the initial values of reference voltages, frequency and phase angle for some fraction of the hour and starts sampling after holding period is over. The reference voltage (v_a^*) is given as the new input to the inverter controller of the DG system. This approach of using sample and hold block allows us to measure the actual change in powers when the output of PV generator changes in the next hour. ζ and β are the gain of the reactive and active power controllers respectively. The initial values of the E_1 and ω_1 are set as 230 Volts and 50 Hz respectively which are the normal operating values in any Indian power system.The detailed description of the system parameters used in the simulation is given in Table II.

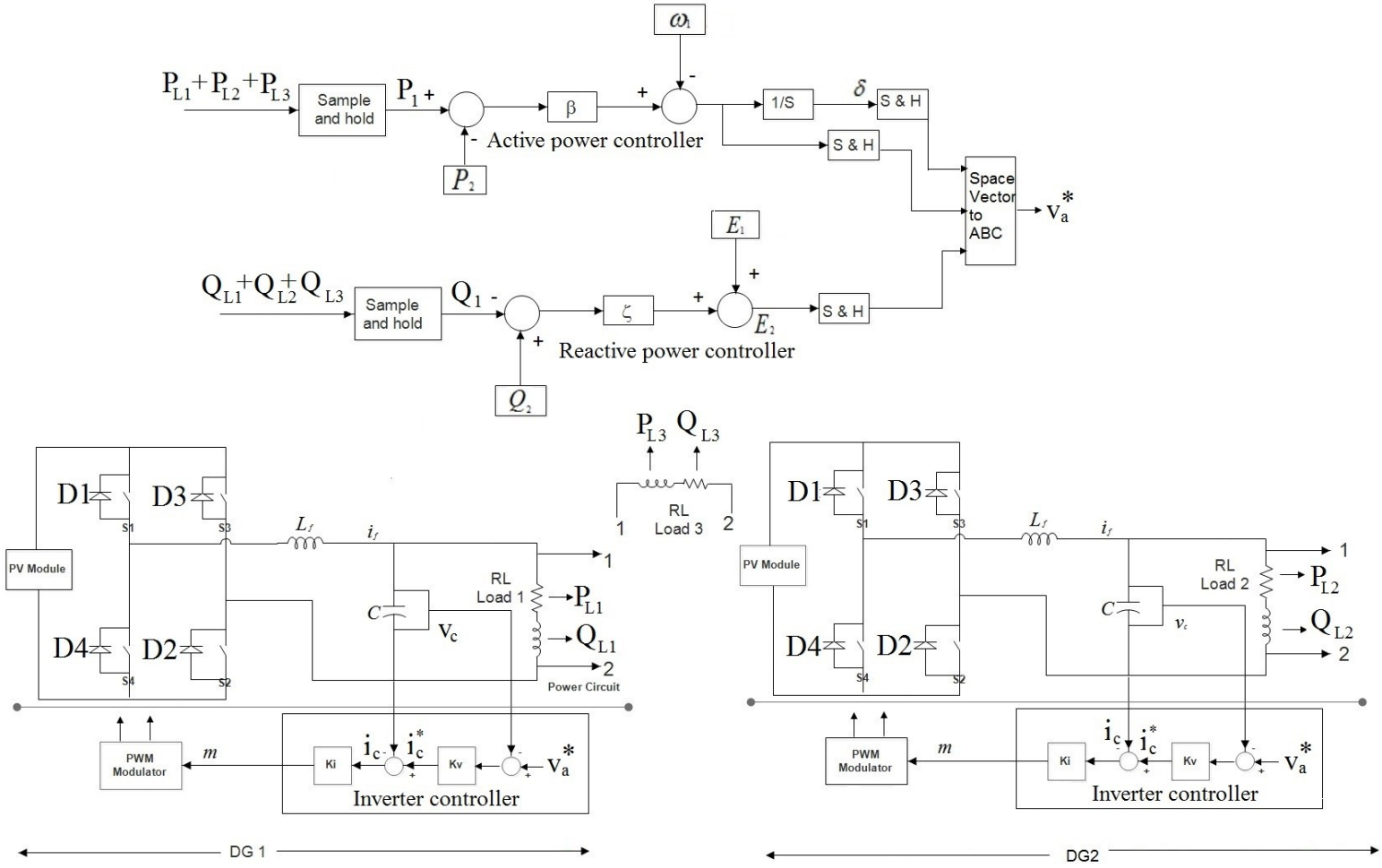

Fig. 29. Schematic representation of single phase microgrid model with controller

TABLE II
SYSTEM PARAMETERS FOR SIMULATIONS

Parameters			Rating
DG System 1	Inverter switching frequency		3 kHz
	Inverter filter inductance		3 mH
	Inverter filter capacitance		150 μF
	PV gen. voltage (standard operating conditions)		300 V
DG System 2	Inverter switching frequency		3 kHz
	Inverter switching frequency		3 mH
	Inverter filter capacitance		150 μF
	PV gen. voltage (standard operating conditions)		300 V
Rating of each DG system			15 KVA
Controller Parameters		ω_1	50 Hz
		ω_{min}	48.5 Hz
		P_2	4.288 kW
		Q_2	3.124 kVAr
		β	-3/560
		ζ	2×10^{-2}
		E_1	230 V
		E_{max}	290 V
Load 1		RL Load (2kW, 1.5 kVAr)	
Load 2		RL Load (2kW, 1.5 kVAr)	
Load 3		RL Load (4kW, 3 kVAr)	

3.9.2 THREE PHASE MICROGRID MODEL WITH CONTROLLER

In the three phase simulation model of microgrid with controller, only one active and one reactive power controller is used as shown in Fig. 30. The three reference values (v_a^*, v_b^*, v_c^*) are generated from the overall configuration of the controller. One reference value is used for each phase of inverter controller. The initial values of the E_1 and ω_1 are again set as 230 Volts and 50 Hz respectively. Three phase R-L loads are used. The sample and hold block operation is same as that is used in the previous section for single phase system. P_1 and Q_1 are the sum of the active and reactive power across the three loads present in the microgrid system. The rest of the model configuration is nearly same as the single phase model while the detailed description of the system parameters is given in Table III.

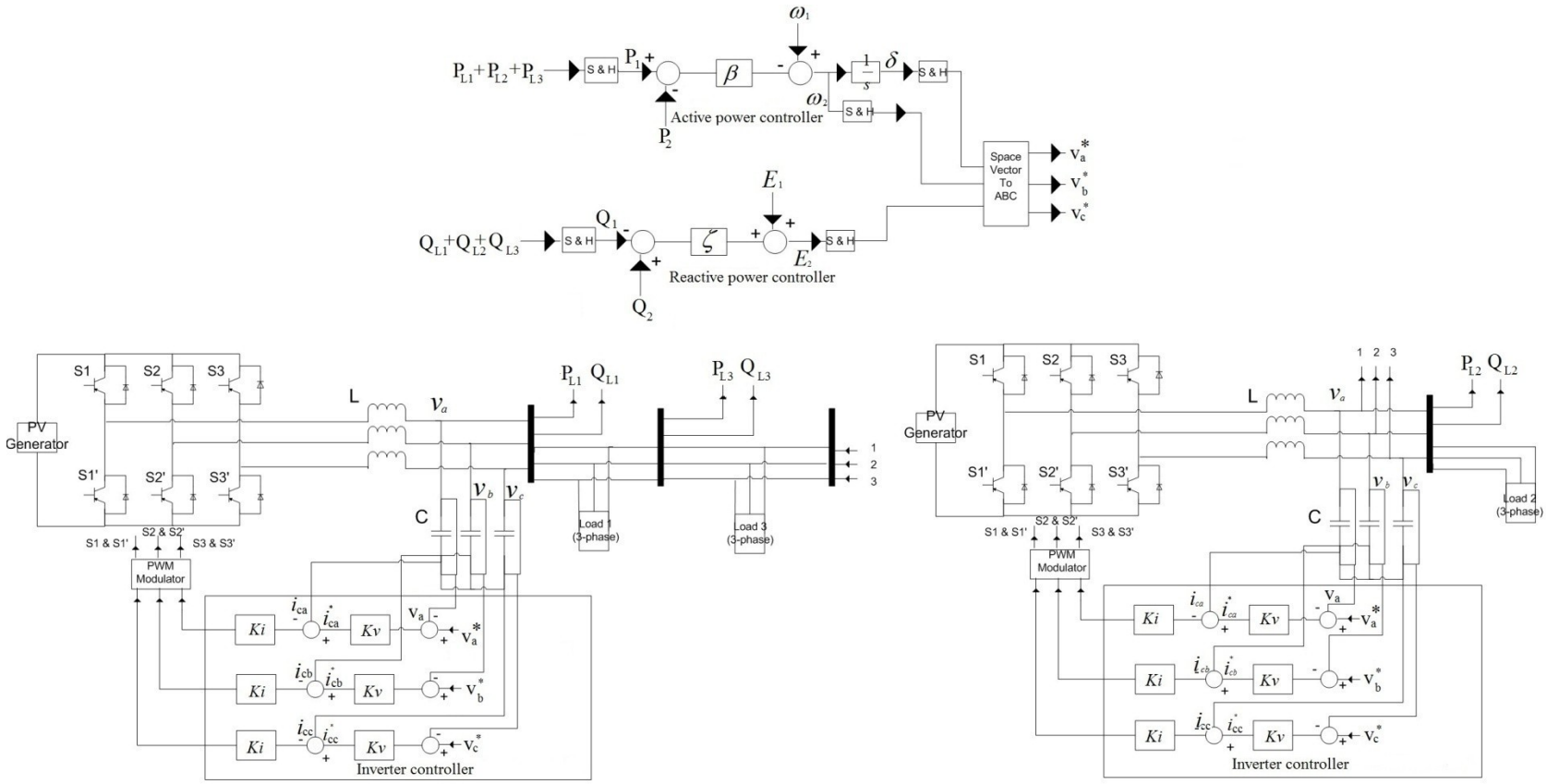

Fig.30 . Schematic representation of three phase simulation model with controller

TABLE III
SYSTEM PARAMETERS FOR SIMULATIONS

Parameters			Rating
DG System 1	Inverter switching frequency		3 kHz
	Inverter filter inductance		3 mH
	Inverter filter capacitance		150 μF
	PV gen voltage (standard operating conditions)		700 V
DG System 2	Inverter switching frequency		3 kHz
	Inverter switching frequency		3 mH
	Inverter filter capacitance		150 μF
	PV gen voltage (standard operating conditions)		700 V
Rating of each DG system			7.85 kVA
Controller Parameters		ω_1	50 Hz
		ω_{min}	48.5Hz
		P_2	8.0 kW
		Q_2	20.0 kvar
		B	-55/36460
		Z	60/470
		E_1	230 V
		E_{max}	290 V
Load 1		RL Load (4kW, 3 kVar)	
Load 2		RL Load (8kW, 6 kVar)	
Load 3		RL Load (4kW, 3 kvar)	

CHAPTER 4

SIMULATION RESULTS AND DISCUSSIONS

In this chapter simulation results of various sub parts of the configuration and of the configurations are discussed in the separate sections and various comments on the waveform outcomes are hence made. All the results are obtained using Simulink in MATLAB 2014.

4.1 SIMULATION RESULTS FOR PV CELL AND GENERATOR

The sample data of the Table I i.e. the eight hour solar insolation and temperature data is represented in Fig. 31 and Fig.32. The solar insolation is nearly 500 W/m^2 and ambient temperature is nearly 34^OC for the first hour, while in the next hour both of these values changes. The maximum solar insolation of 819.93 W/m^2 occurs in between 3-4 hours and maximum temperature of 44^OC occurs between 5-6 hours as shown in the following Fig. 31 and 32 respectively. The above sample data of solar insolation and temperature is then given as the input to the PV cell while no shaded cell in the module is considered. Under the influence of the above data the open circuit voltage and Short circuit current of the PV cell (which was modelled in section 3.3) changes as according to their governing equations explained earlier, shown in Fig. 33 and Fig 34.

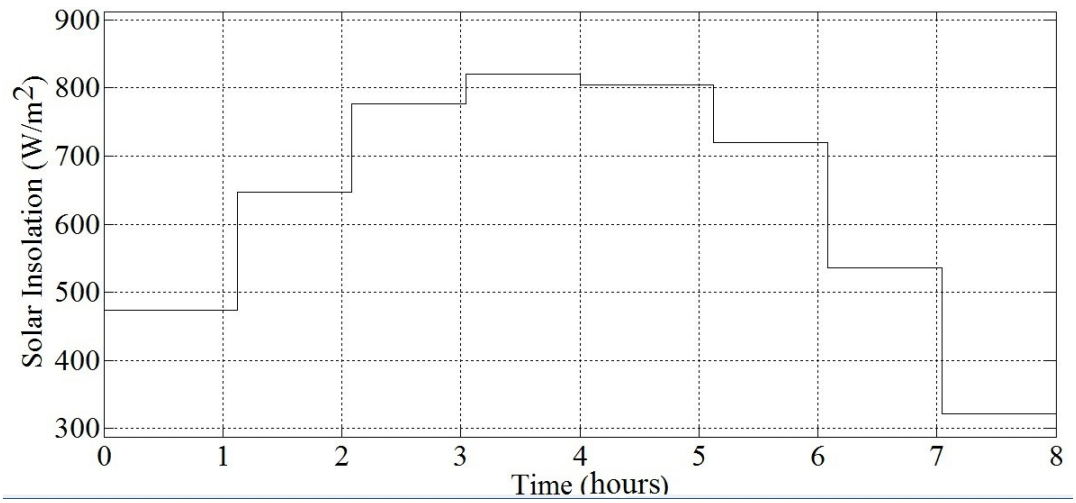

Fig. 31. Solar Insolation levels of PV cell for eight hours

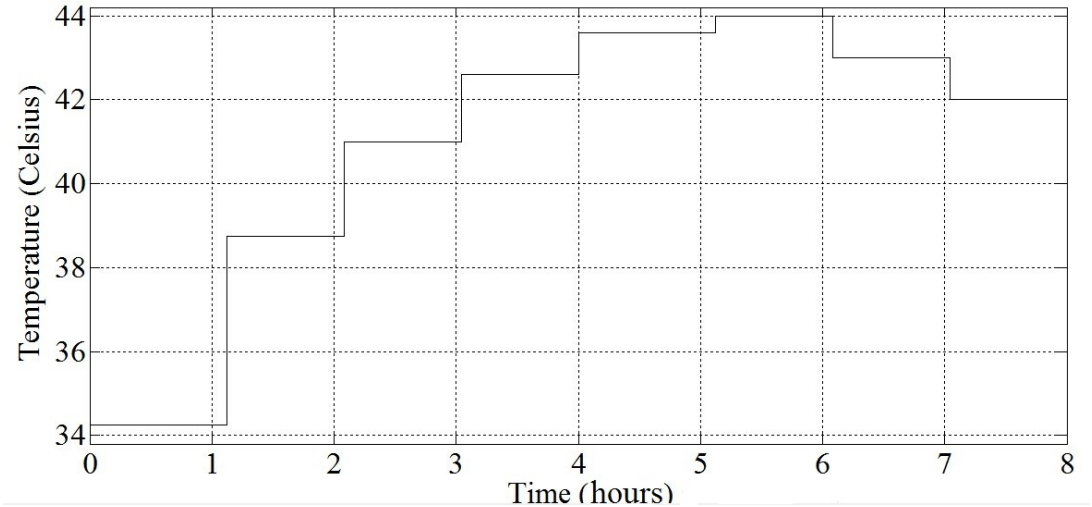

Fig. 32. Temperature levels of the PV cell for eight hours

The maximum open circuit voltage of the PV cell i.e. 0.475 Volts occurs in 0-1 hour because the ambient temperature is lowest at 34.25^{O}C afterwards the O.C voltage keep on decreasing and reaches a lowest of 0.45 Volts between 4-5 hour. While the response of the short circuit current of the PV cell largely depends upon the solar insolation level hence the S.C current waveform of the PV cell shown in Fig. 34 is similar in shape with the Fig. 31. The maximum S.C current achieved is nearly 1.6 Amperes during 3-4 hour while the S.C. current of the cell is 3.896 Amperes during STC.

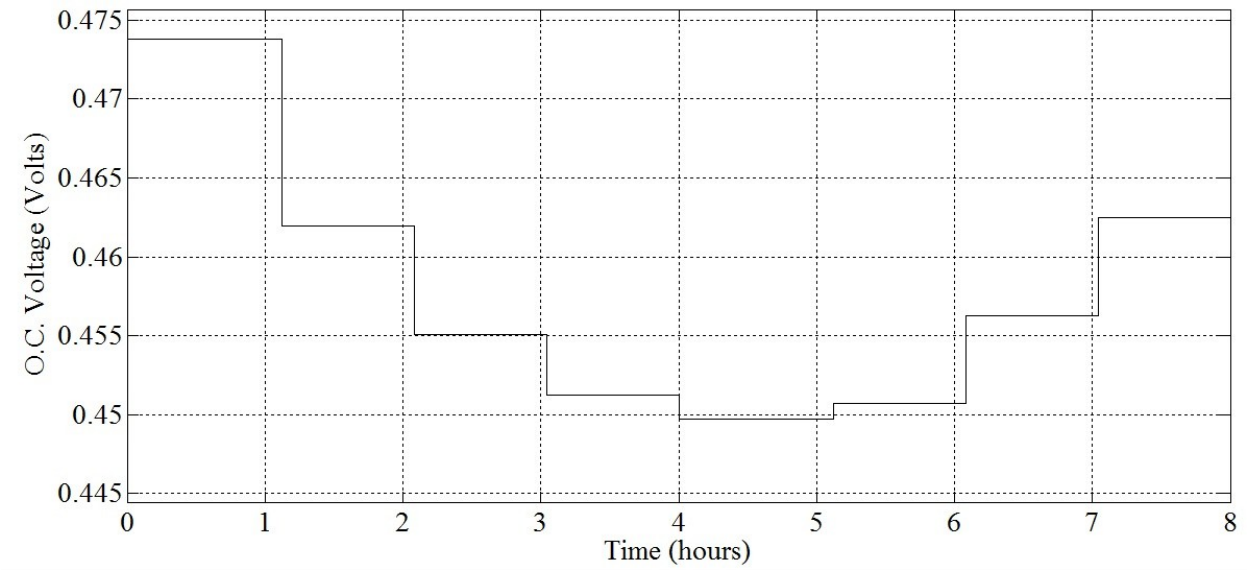

Fig. 33. Open Circuit Voltage of PV cell

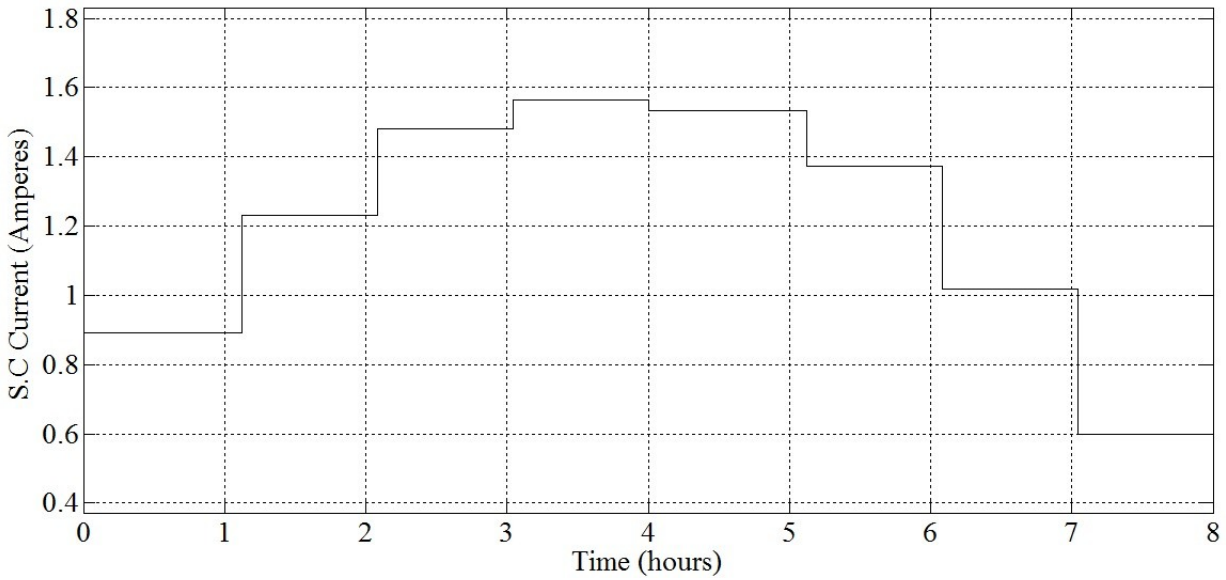

Fig. 34. Short circuit current of PV cell

The array configurations of the PV generators for both single phase and three phase are already explained in the previous sections, however, the response of the open circuit voltage of both these generators under the sample data of Table I is shown in Fig. 36 and Fig. 37. The O.C voltage response for both the single phase and three phase generator is similar to the O.C voltage response of the PV cell. The maximum voltage achieved for single phase PV generator is 296 Volts and is 698 Volts for three phase generator, while the minimum voltage is 282 and 663 Volts respectively. Now according to the equation (21) in section 3.4, when the reference voltage changes the output voltage of the inverter also changes. The output RMS voltage across load 1 in Fig. 23 is recorded and is shown in Fig. 35. The output voltage across the inverter also shows the similar curve nature of curve as that of the O.C voltage of the single phase PV generator hence proving equation 21 graphically.

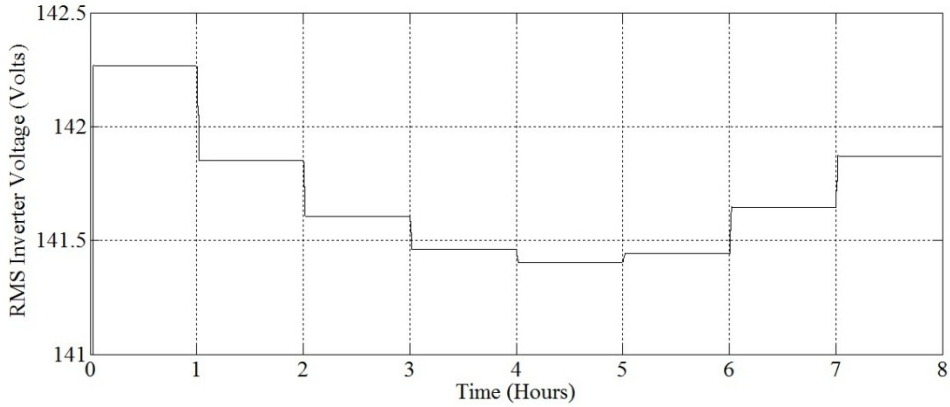

Fig. 35. RMS Inverter voltage for single phase microgrid model

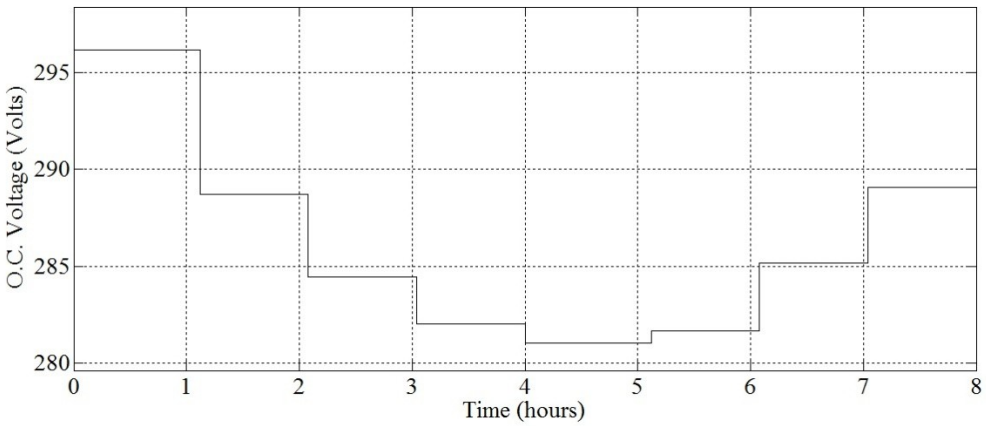

Fig. 36. Open circuit voltage of single phase PV generator

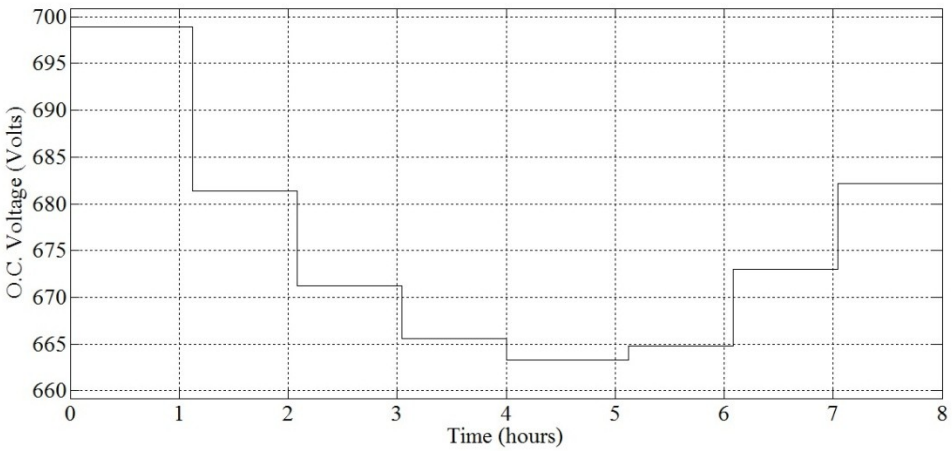

Fig. 37. Open circuit voltage of three phase PV generator

The I-V curves of the PV cell for varying irradiance level and temperature is given in Fig. 38 and Fig. 39 respectively. The short circuit current varies in direct proportion to the irradiance level while the open circuit voltage changes by 0.37 % for each degree rise in temperature.

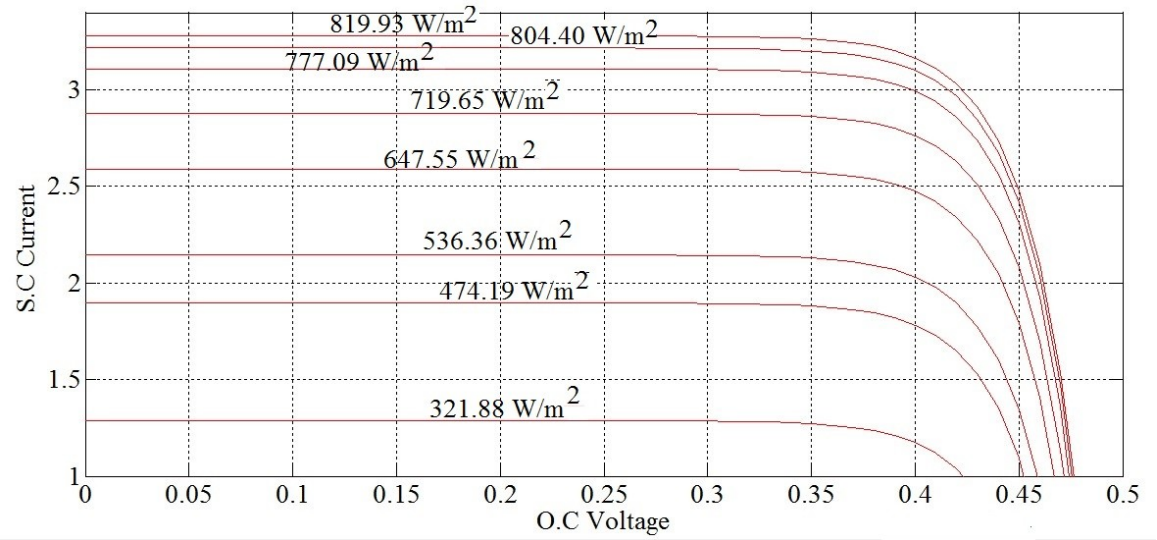

Fig. 38 PV cell I-V curve for varying irradiance level

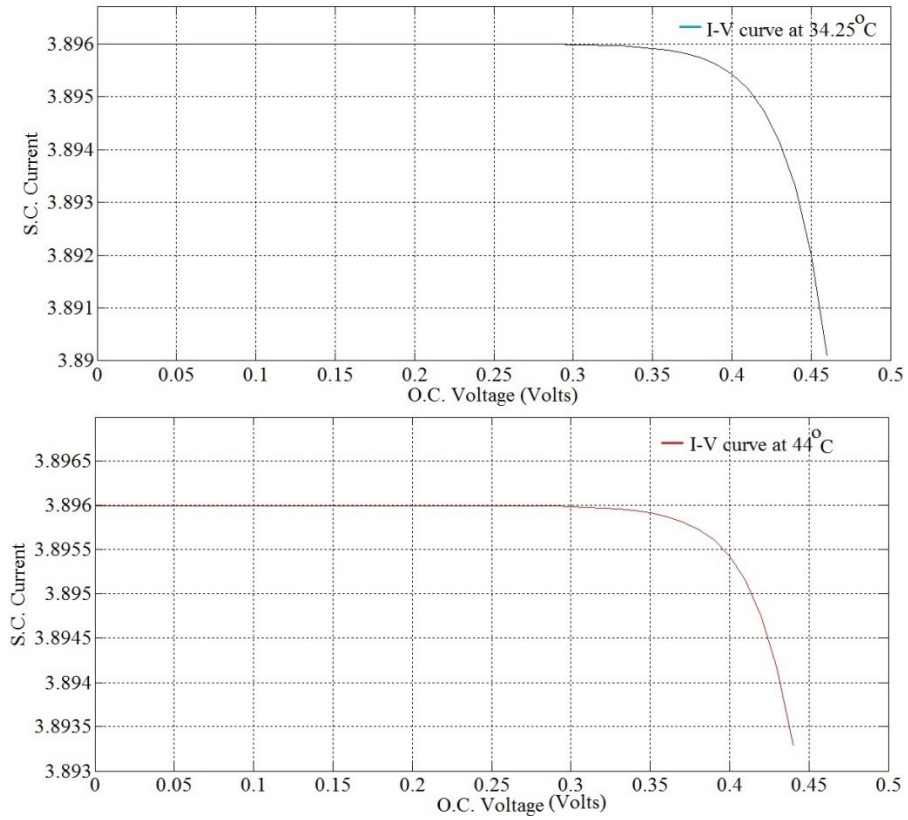

Fig. 39 Comparison of I-V curve at two different temperatures (highest and lowest)

4.2 SIMULATION RESULTS OF MICROGRID MODEL WITHOUT CONTROLLER

The microgrid model of both the single phase (Fig. 23) and three phase (Fig. 24) as in section 3.7 are simulated based on the sample data of Table I without any controlling action of active or reactive power. Hence, recordings of both the active and reactive power across the three loads are presented in the microgrid configuration for eight hours in Fig 40 and Fig. 41 for single phase model and in Fig. 42 and Fig. 43 for three phase model respectively.

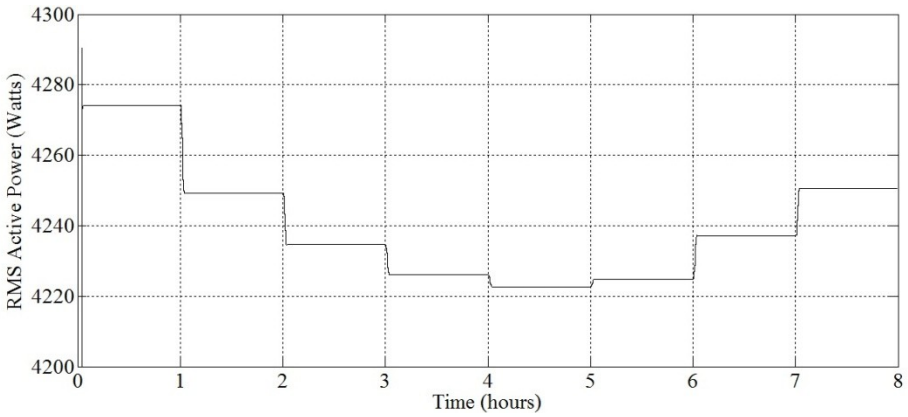

Fig. 40. RMS active Power across three loads for single phase microgrid model

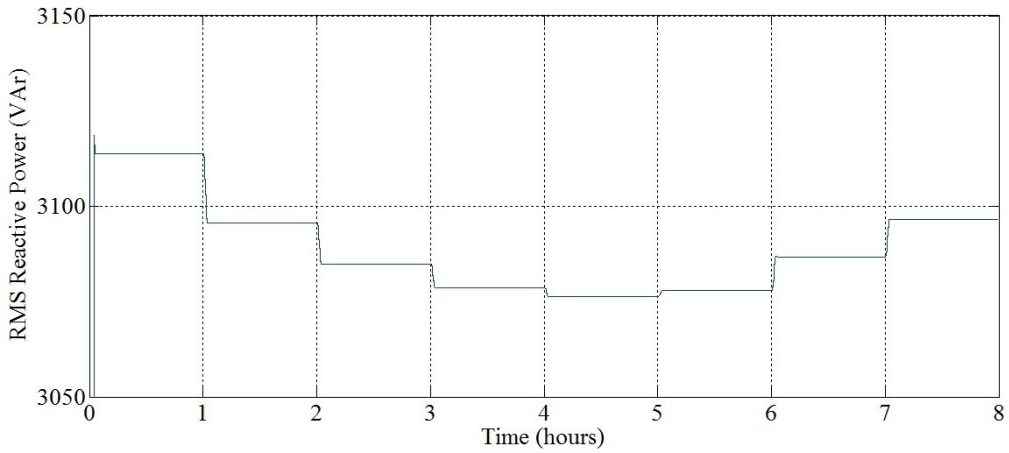

Fig. 41. RMS reactive power across three loads for single phase microgrid model

The active and reactive power across the loads in single phase model is maximum during 0-1 hour and drops to its minimum during the 4-5 hour and then again starts rising in the next hours. Both the powers are showing the unwanted drop which is an undesirable phenomenon in any

system. The nature of response for three phase model response is also similar to single phase model but the magnitude for the latter case is different.

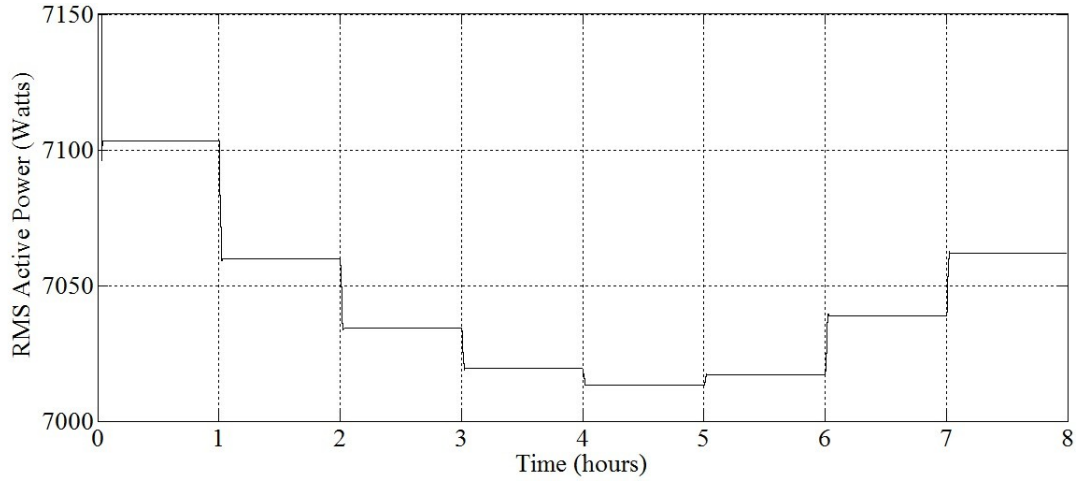

Fig. 42. RMS active power across three loads for three phase microgrid model

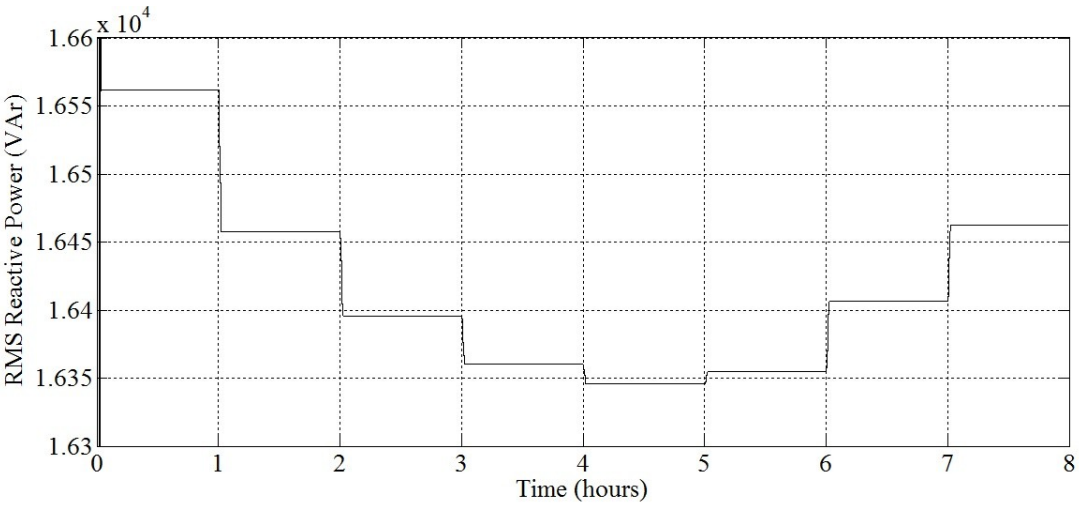

Fig. 43. RMS reactive power across three loads for three phase microgrid model

The above active and reactive power variations for single phase and three phase microgrid model depicts the fall in the active and reactive power across the loads as the solar insolation and temperature input levels of the PV generator changes.

4.3 SIMULATION RESULTS FOR MICROGRID MODEL WITH PROPOSED CONTROLLER

The model of the microgrid (Fig. 29 and Fig. 30) is now simulated in the presence of the active and reactive power controllers which are explained earlier in section 3.9. The controllers help to uplift the active and reactive power to their desired values during operation of the PV generator. The RMS voltage observed across the Load1 in Fig. 28 with and without controller is shown in Fig. 44. This figure depicts the improvement in voltage profile across the load when the proposed controller is used for the same configuration. The comparison of the active and reactive power across the loads with and without controller is depicted in Fig. 45 and Fig. 46 for single phase microgrid model and in Fig. 47 and Fig. 48 for three phase microgrid model.

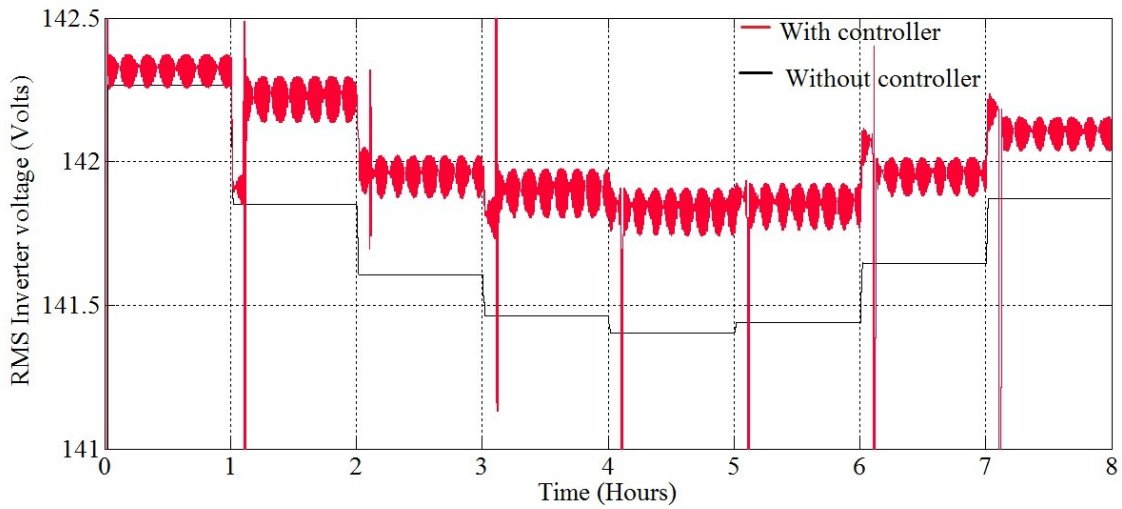

Fig. 44. Comparison of the RMS Inverter voltage with and without controller for single phase microgrid model

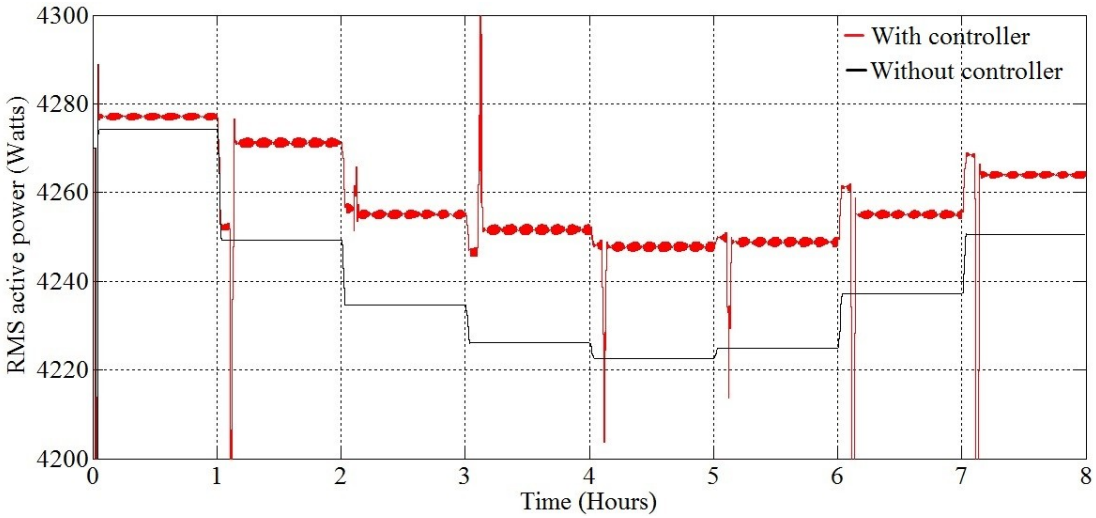

Fig. 45. Comparison of active power with and without controller for single phase microgrid model

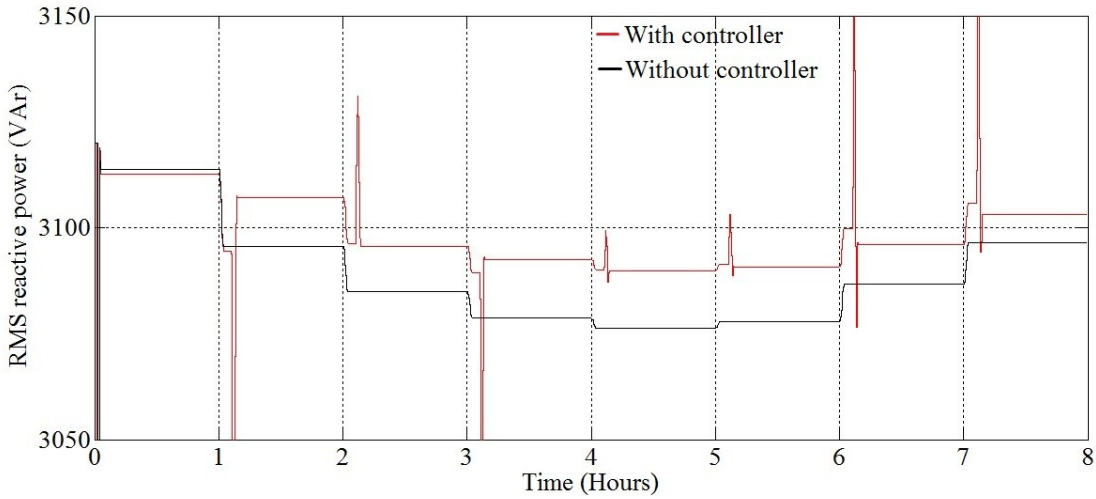

Fig. 46. Comparison of reactive power with and without controller for single phase microgrid model

As depicted in Fig. 45 and Fig. 46 after the sampling period is over, the controller tries to bring back the active and reactive power to its desired value. The working of the controllers is already explained in the previous chapter. The lowest RMS active power without controller is 4230 Watts and when the controller is used the lowest active power is uplifted to 4250 Watts. Similarly, for three phase simulation these values are 7340 Watts without controller and 7440 Watts with controller respectively as depicted in Fig. 47. In the same fashion the controllers also

uplift the minimum RMS reactive power from 3075 VAr to 3090 VAr for single phase model and from 17.20 KVAr to 17.35 KVAr for three phase model which is shown in Fig. 48.

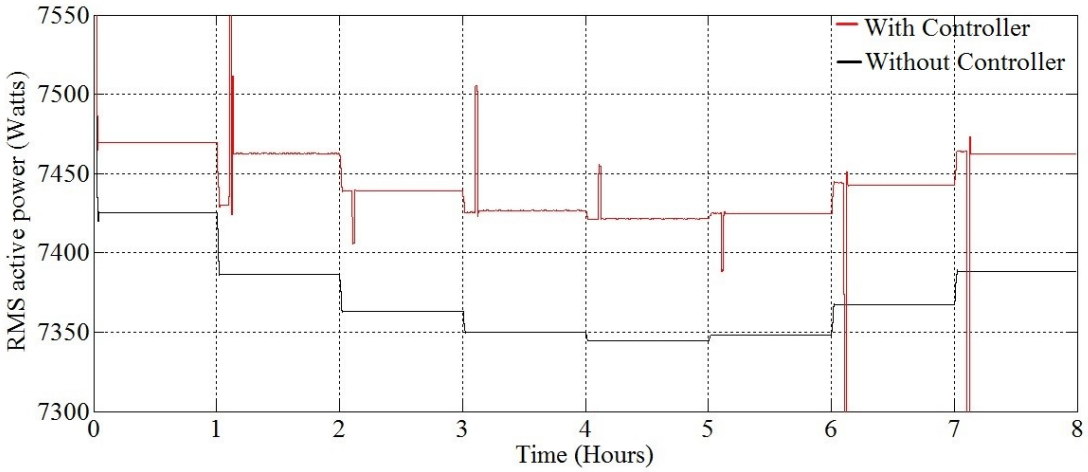

Fig. 47. Comparison of active power with and without controller for three phase microgrid model

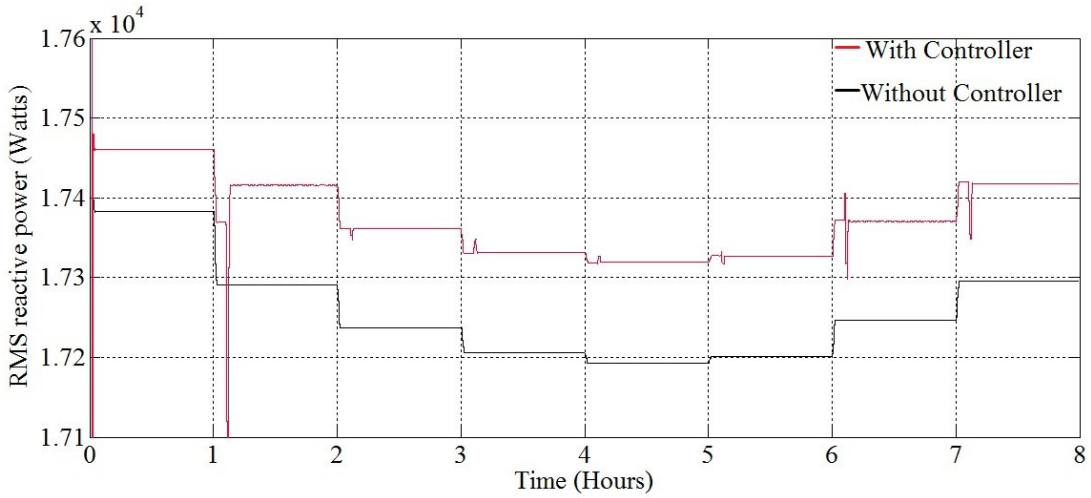

Fig. 48. Comparison of reactive power with and without controller for three phase microgrid model

CHAPTER 5
CONCLUSIONS AND FUTURE SCOPE

This dissertation work presents the importance of actual model of PV generator instead of using a constant dc source in various studies for control strategies of solar microgrid. The PV generator is simulated on the bases of the sample data collected from the weather station at Patiala [23]. The microgrid proposed in this dissertation work has the provision for application of data related to solar irradiance, ambient temperature and shading effect collected from other location too. The inverter open circuit voltage and short circuit current have shown the noticeable changes due to which the active and reactive power dissipated across the loads also change in the microgrid system. Any unwanted drop in the power is undesirable in any kind of power system, so the power controller based on the power loops is used and its operation is described. The proposed controller has the ability to bring back the active and reactive power up to the desired level by controlling the magnitudes of voltage and frequency comparing of the reference signal of the inverter controller in the islanded mode of the microgrid. Under this condition the PV generator operates on the practical consideration of the temperature and solar insolation levels. In the proposed microgrid configuration the same controller is used to obtain the improved results for active and reactive power across the loads. The simulations results confirmed the effective working of the controller in the islanded mode of operation of the microgrid. The dissertation work describes how the solar microgrids, which can operates in the remote areas where no connection to the utility grid is possible, can be made more efficient while operating in the changing weather parameters to which the PV cell/array is exposed.

In the future work, the proposed microgrid can be simulated with more number of DG sources and higher rating loads which can be installed for that configuration. Four to five number of DG sources may be considered for this kind of study. Another important aspect which could be carried out on the same research platform is the replacement of one or more PV generator with some other different types of microsource such as wind generator model, fuel cell model or bio gas steam engine coupled generator. The different nature of operational characteristics should be considered for proper modelling of microgrid using Simulink. Finally, the overall approach of this dissertation may be effective for performance analysis of a solar microgrid at R&D level.

LIST OF PUBLICATIONS

[1] Pankaj Verma, Prasenjit Basak, Microgrids: Opening New Possibilities for the Electricity Grid , Akshay Urja, Volume 9, Issue 5, pp 12-15, April 2016, MNRE, Government of India, published by TERI- The Energy and Resource Institute, Lodhi Road, New Delhi.

[2] Pankaj Verma, Prasenjit Basak, "Active and reactive power control using droop characteristics controller in a microgrid," 2016 IEEE 7th India International Conference on Power Electronics-Thapar University, Patiala November 17-19 (**Communicated on May 25, 2016**).

[3] Pankaj Verma, Prasenjit Basak, "Programming based study of shading effect in a photovoltaic array," International journal of Advanced Research in Electrical, Electronics and Instrumentation Engineering. (**Communicated on July 12,2016**)

REFERENCES

[1] Hubbert's upper-bound prediction for US crude oil production (1956), and actual lower-48 states production through 2014 available on https://en.wikipedia.org/wiki/Hubbert_peak_theory.

[2] Tu Yiyun; Li Can; Cheng Lin; Le Lin, "Research on Vehicle-to-Grid Technology", Computer Distributed Control and Intelligent Environmental Monitoring (CDCIEM), 2011 International Conference on year 2011.

[3] Jinwei He, Student Member, IEEE, Yun Wei Li, Senior Member, IEEE, Josep M. Guerrero, Senior Member, IEEE, Frede Blaabjerg, Fellow, IEEE, and Juan C. Vasque, "An Islanding Microgrid Power Sharing Approach Using Enhanced Virtual Impedance Control Scheme," IEEE transactions on power electronics, vol. 28, no. 11, november 2013.

[4] Y. W. Li, D. M. Vilathgamuwa, and P. C. Loh, "Microgrid Power Quality Enhancement Using Three-Phase Four-Wire Grid-Interfacing Compensator," IEEE transactions on industry applications, vol. 41, no. 6, pp. 1707-1719, Nov. 2005.

[5] Xisheng Tang, Wei Deng and Zhiping Qi, "Research on Micro-grid Voltage Stability Control Based on Supercapacitor Energy Storage," Institute of Electrical Engineering of Chinese Academy of Sciences, Beijing, China.

[6] Jinwei He, and Yun Wei Li, "An Accurate Reactive Power Sharing Control Strategy for DG Units in a Microgrid," 8th international conference on power electronics – ECCE Asia May 30-June 3 , 2011, The Shillu jeju, Korea.

[7] Yaoqin Jia, Dingkun Liu and Jia Liu, "A Novel Seamless Transfer Method for a Microgrid Based on Droop Characteristic Adjustment," 2012 IEEE 7th International Power Electronics and Motion Control Conference - ECCE Asia June 2-5, 2012, Harbin, China.

[8] Y. W. Li, D. M. Vilathgamuwa, and P. C. Loh, "Design, analysis and realtime testing of controllers for multi-bus micro-grid system," IEEE Trans. Power Electron., vol. 19, no. 5, pp. 1195–1204, Sep. 2004.

[9] David Bakken, Krzysztof Iniewski, "Microgrids," in Smart Grids (clouds, communications, open source, and automation), Washington State University.

[10] Microgrids from data centers to developing countries, an enticing solution for self-sufficient power, January 2012. Available at: http/www.lead-central.com/AssetManager/e0bc9e75-84f1-4cal-9c65-21c74a8b75fe/Documents/New%20WP%20file/ABB-73-WPO_Microgrids.pdf.

[11] Ashraf Khalil, Khalid Ateea Alfaitori and Ali Asheibi, "Modellind and control of PV/wind microgrid," 7th International Renewable Energy Congress (IREC) 2016 pp 1-6 DOI: 10.1109/IREC.2016.7478916.

[12] P E S N Raju; Trapti Jain, "Centralized Supplementary Controller to Stabilize an Islanded AC Microgrid," Power Systems Conference (NPSC), 2016 Eighteenth National, 2014 pp 1-6 DOI: 10.1109/NPSC.2014.7103800

[13] Yixin Zhu; Fang Zhuo; Feng Wang; Baoquan Liu; Ruifeng Gou; Yangjie Zhao, " A virtual impedance optimization method for reactive power sharing in networked microgrid," IEEE Transactions on Power Electronics Volume: 31, Issue: 4 pp 2890 – 2904 2016

[14] Yun Zhang, Le Xie,Member and Qifeng Ding, "Interactive Control of Coupled Microgrids for Guaranteed System-Wide Small Signal Stability," IEEE transactions on smart grid, Vol. 7, No. 2, march 2016

[15] Morad Mohamed Abdelmageed Abdelaziz, Hany E. Farag, and Ehab F.El-Saadany, "Optimum Reconfiguration of Droop-Controlled Islanded Microgrids," IEEE transactions on power systems, vol.31, no.3, may2016

[16] Li Bin; Zhou Lin; Yu Xirui; Zheng Chen; Liu Jinhong; Xie Bao, "New Control Scheme of power Decoupling Based on Virtual Synchronous Generator," IEEE Power and Energy Conference at Illinois (PECI) 2016 DOI: 10.1109/PECI.2016.7459257

[17] N. M. Abdel-Rahim and J. E. Quaicoe, "Analysis and design of a multiple feedback loop control strategy for single-phase voltage-source UPS inverters," IEEE Trans. Power Electron., vol. PE-11, pp. 532–541, July 1996

[18] N. Abdel-Rahim and J. E. Quaicoe, "Three-phase voltage-source UPS inverter with voltage-controlled current-regulated feedback control scheme," in Proc. 20th Int. Conf. Industrial Electronics, Control, and Instrumentation (IECON'94), vol. 1, 1994, pp. 497–502.

[19] Kawamura, A., Haneyoshi, T., and Hoft, R. C., "Dead Beat Controlled PWM Inverter with Parameter Estimation Using Only Voltage Sensar,"IEEE Power Eleetronicr Speciolistr Conference (PESC), pp. 576583, 1988.

[20] Wind energy program in India, www.inwea.com, available on http://www.inwea.org/aboutwindenergy.htm

[21] Solar power in Inda, www.wikipedia.org, available on https://en.wikipedia.org/wiki/Solar_power_in_India

[22] Gilbert M. Masters, "Photovoltaic materials and electrical characteristics," Renewable and efficient electric power systems, Stanford University.

[23] Souvik Ganguli and Jasvir Singh, "Estimating the Solar Photovoltaic generation potential and possible plant capacity in Patiala," in International Journal Of Applied Engineering Research, Dindigul, vol. 1 No. 2 , 2010, pp. 253-260.

[24] N. Abdel-Rahim and J. E. Quaicoe, "Three-phase voltage-source UPS inverter with voltage-controlled current-regulated feedback control scheme," in Proc. 20th Int. Conf. Industrial Electronics, Control, and Instrumentation (IECON'94), vol. 1, 1994, pp. 497–502

[25] B.S. Manke, " Stability analysis of control systems," Linear control systems

CURRICULUM VITAE OF AUTHOR

1. Personal information

Name : Pankaj Verma

Fathers Name : Om Parkash Verma

Date of Birth : 14/08/1991

Languages Known : English, Hindi and Punjabi

Email: bluepankaj123@gmail.com

2. Academic Qualifications

Course	Board/ University	Percentage	Year of passing
B.Engg. in electrical & electronics	Panjab university, chandigarh	75 %	2013
12^{th}	CBSE	80 %	2009
10^{th}	CBSE	84.2 %	2007
M.E in power systems(till 3^{rd} Sem)	Thapar University	78%	2016

3. List of Publications

[1] Pankaj Verma, Prasenjit Basak, Microgrids: Opening New Possibilities for the Electricity Grid , Akshay Urja, Volume 9, Issue 5, pp 12-15, April 2016, MNRE, Government of India, published by TERI- The Energy and Resource Institute, Lodhi Road, New Delhi.

PLAGIARISM CERTIFICATE

Pankaj_thesis

ORIGINALITY REPORT

14%	5%	11%	4%
SIMILARITY INDEX	INTERNET SOURCES	PUBLICATIONS	STUDENT PAPERS

PRIMARY SOURCES

1	Masters. "Photovoltaic Materials and Electrical Characteristics", Renewable and Efficient Electric Power Systems, 07/28/2004 Publication	2%
2	J.E. Quaicoe. "Multiple feedback loop control strategy for single-phase voltage-source UPS inverter", Proceedings of 1994 Power Electronics Specialist Conference - PESC 94 PESC-94, 1994 Publication	1%
3	www.edi-info.ir Internet Source	1%